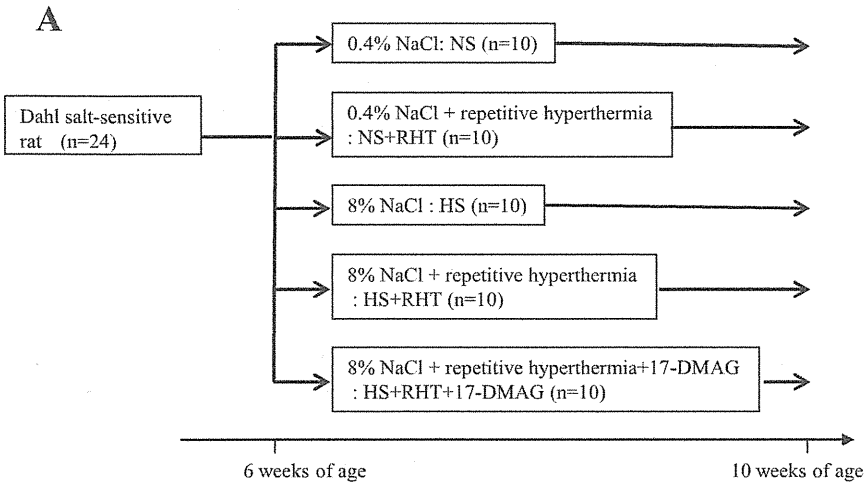

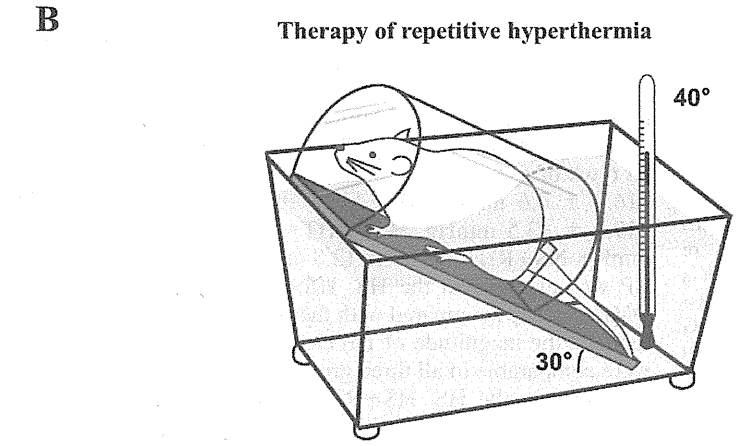

Fig. 1. *A*: study time line. *B*: scheme of rat immersion in a hot water bath in the HS+RHT group. NS, normal salt; HS, high salt; RHT, repetitive hyperthermia.

ducer. M-mode echocardiograms were recorded in the short-axis view at the papillary muscle level of the LV at a speed of 100 mm/s for measurement of LV end-diastolic (LVDd) and end-systolic (LVDs) diameters, LV fractional shortening (FS), and the thickness of the intraventricular septum (IVS) and LV posterior wall (PW) at end diastole. The following variables were determined as indicators of diastolic ventricular function: peak transmitral flow velocity in early diastole (E), peak transmitral flow velocity in late diastole (A), the E-to-A ratio (E/A), and deceleration time of the E wave. After echocardiography, a 1.4 F micromanometer-tipped catheter (Millar Instruments, Houston, TX) was inserted into the right carotid artery and then advanced into the LV to measure pressure. After the hemodynamic studies, the heart was immediately harvested. Body weight, heart weight calibrated by tibia length, and the ratio of heart weight to body weight as an index of cardiac hypertrophy were evaluated.

Histological examination. The apical portion of the LV below the papillary muscle was fixed with phosphate-buffered 10% formalin solution for 24 h, embedded in paraffin, sectioned at 1.5 μm, and stained with hematoxylin-eosin (HE), Masson's trichrome (MT), or Sirius red (SR) to evaluate the cardiac fibrosis and hypertrophy of cardiomyocytes. To determine myocyte cross-sectional area (CSA), 30 cardiomyocytes were traced in each section in the slides stained with HE using NIH Image software. The percentage area of perivascular and interstitial fibrosis in the LV at the papillary muscle level in the slides stained with MT and SR was determined (6, 8). The remaining LV was immediately placed in liquid nitrogen and stored at −80°C for Western blot analyses.

Myocardial metalloproteinase activity assay. The SensoLyte 520 Generic MMP Fluorometric Assay Kit (AnaSpec) was used to determine myocardial matrix metalloproteinase (MMP) activity according to the manufacturer's directions. Hearts were homogenized in the assay buffer and incubated with 1 mmol/l of 4-aminophenylmercuric acetate for 24 h at 37°C to activate pro-MMPs. Data were adjusted by protein concentrations in the buffers and normalized to the levels in the NS group.

Analysis of protein expression. Frozen heart tissues were homogenated with 5 volumes of homogenization buffer (RIPA) and centrifuged at 15,000 rpm for 20 min. The protein concentration of the supernatant was determined with bovine serum albumin as a standard protein. The same amount (20 g for each experiment) of extracted protein was loaded for SDS-polyacrylamide gel electrophoresis and then transferred onto polyvinylidene difluoride membranes. Membranes were blocked and incubated with antibodies against endothelial nitric oxide synthase (eNOS) (sc-20791, Santa Cruz Biotechnology), phosphor-eNOS (N213220; NOF Medical Department, Tokyo, Japan), Akt (#9272, Cell Signaling Technology), phospho-Akt (#9271, Cell Signaling Technology), HSP60 (SPA-806, Stressgen), HSP70 (SPA-810, Stressgen), HSP90 (SPA-845, Stressgen), brain natriuretic peptide (BNP) (SC-18818, Santa Cruz Biotechnology), inducible nitric oxide synthase (iNOS) (SC-650, Santa Cruz Biotechnology), nitrotyrosin (905-763-100, Stressgen), pentraxin 3 (PTX3) (H00005806-MO2, Abnova), Toll-like receptor (TLR)-4 (IMG-578A, IMGENEX), telomere reverse transcriptase (TERT) (SC-7212, Santa Cruz Biotechnology), Sirt1 (SC-15404, Santa Cruz Biotechnology) and to glyceraldehyde-3-phosphate-dehydrogenase (GAPDH: sc-20357, Santa

Cruz Biotechnology). Detection was performed with secondary horseradish peroxidase-conjugated antibodies (Millipore, Billerica, MA) and the ECL detection system. Subsequently, the signals were normalized to GAPDH expression. To assess the level of myocardial oxidative stress generated in the process of cardiac remodeling, we determined the degree of lipid peroxidation in myocardial tissues through biochemical assay of thiobarbituric acid reactive substances (TBARS) (31). Briefly, LV myocardial tissue was homogenized (10% wt/vol) in 1.15% KCl solution (pH 7.4). The homogenate was mixed with 0.4% SDS, 7.5% acetic acid adjusted to pH 3.5 with NaOH, and 0.3% thiobarbituric acid. Butylated hydroxytoluene (0.01%) was added to the assay mixture to prevent autoxidation of the sample. The mixture was kept at 5°C for 60 min and was heated at 100°C for 60 min. After cooling, the mixture was extracted with distilled water and *n*-butanol-pyridine (15:1, vol/vol) and centrifuged at 1,600 *g* for 10 min. The absorbance of the organic phase was measured at 532 nm. The amount of TBARS was determined by absorbance with the molecular extinction coefficient of 156,000 and expressed as mol/g wet wt.

Telomeric biology. To extract the genomic DNA, the tissue samples were lysed by incubation at 55°C for 48 h in 200 μl lysis buffer containing 10 mmol/l Tris·HCl (pH 8.0), 0.1 mmol/l EDTA (pH 8.0), 2% SDS, and 500 μg/ml protease K (Roche Diagnostic, Tokyo, Japan). Genomic DNA extraction was performed using a DNeasy Tissue kit (Qiagen, Tokyo, Japan) according to the manufacturer's recommendations as previously described (6). The length of the telomeric DNA was estimated as the telomeric-to-centromeric DNA content ratio, as previously reported (16). The telomeric DNA contents can be standardized by calculating the relative telomeric DNA content with the centromeric DNA (0.1 μg) content. DNA samples were diluted and denatured. Two microliters of denatured DNA were dotted onto a nylon membrane sheet. The hybridization signal of a digoxigenin (DIG)-labeled probe was converted into a chemiluminescent signal using a DIG Wash and Block buffer set, and a DIG luminescent detection kit (Roche). After the telomere probe had been stripped, the membrane was rehybridized with 2 pmol 5′-DIG-labeled centromere-specific oligonucleotide (5′-GTTTTGAAACACTCTTT-TTGTAGAATCTGC-3′) under the same conditions. The telomere probe was visualized by alkaline phosphatase-metabolizing CDP-Star, a highly sensitive chemiluminescence substrate. Telomerase activity was examined by means of a modified telomerase repeat amplification protocol (TRAP) with TeloChaser (Toyobo, Osaka, Japan) according to the manufacturer's instructions (16). Briefly, the substrate oligonucleotide is added to 0.5 g protein extract. If telomerase is present and active, telomeric repeats (GGTTAG) are added to the 3′-end of the oligonucleotide. After amplification, the PCR products were resolved on a 12% polyacrylamide gel, stained with ethidium bromide, and detected using an FLA 5000 system (Fuji Film, Tokyo, Japan). The intensities of the bands were quantified with Image J. Assays were repeated at least twice on LV tissue from each animal to ensure reproducibility. A human cancer cell line overexpressing telomerase was used as the reference in each assay.

Additional methods. The expanded METHODS section in the online-only Data Supplement contains information of the heat-induced lowering effects of blood pressure (BP) by hyperthermia.[1]

Data analysis. Data are presented as means ± SE. The differences in a single parameter among the groups were evaluated by one-way analysis of variance using the Bonferroni post hoc test for multiple comparisons. A P value of < 0.05 was considered to be statistically significant.

RESULTS

Hemodynamic and morphological analyses. Body weight was significantly lower in the HS and HS+RHT groups than in the NS group. Heart weight calibrated by tibia length and the ratio of heart weight to body weight, an index of cardiac hypertrophy, were both significantly increased in the HS group compared with those in the NS and HS+RHT groups (Table 1). At 6 wk of age, SBP was similar among the three groups (NS: 116.0 ± 6.6 mmHg, HS: 118.5 ± 17.7 mmHg, HS+RHT: 119.0 ± 13.5 mmHg, HS+RHT+17-DMAG: 115.7 ± 11.2 mmHg, NS+RHT: 118.4 ± 12.8 mmHg). At 10 wk of age, the BP was elevated in the HS, HS+RHT, and HS+RHT+17-DMAG groups compared with the NS group, but hyperthermia reduced the magnitude of BP elevation (Table 1). Heart rates were comparable in all three groups. LV end-diastolic pressure (LVEDP) in the HS, HS+RHT, and HS+RHT+17-DMAG groups was significantly higher than that in the NS group; however, LVEDP in the HS+RHT group was reduced compared with that in the HS group. In the HS, HS+RHT, and

[1] The online version of this article contains supplemental material.

Table 1. *Hemodynamic and echocardiographic measurements at 10 wk*

Parameter	NS	HS	HS + RHT	HS + RHT + 17-DMAG	NS + RHT
n	10	10	10	10	10
BW, g	368.3 ± 2.7	291.5 ± 8.6**	299.8 ± 7.9**	302.0 ± 10.8**	360.5 ± 6.4##++$$
HW/tibia length, mg/mm	24.32 ± 1.05	42.11 ± 2.30**	29.24 ± 1.09##	38.05 ± 3.11**+	24.38 ± 1.30##$$
HW/BW, mg/g	3.27 ± 0.12	6.89 ± 0.41**	5.00 ± 0.16**##	6.24 ± 0.54**	3,46 ± 0.13##+$$
Systolic BP, mmHg	126.3 ± 2.2	202.6 ± 5.3**	169.9 ± 3.3**##	179.6 ± 5.3**##	123.6 ± 3.3##++$$
HR, bpm	391.5 ± 6.5	417.5 ± 11.8	392.5 ± 18.9	414.3 ± 17.7	390.8 ± 12.1
LVEDP, mmHg	4.6 ± 0.8	15.5 ± 0.7**	11.4 ± 0.8**#	13.9 ± 0.8**++	5.1 ± 0.9##$$
			Echocardiographic data		
LVDd, mm	6.44 ± 0.08	5.40 ± 0.09**	5.88 ± 0.14*#	5.65 ± 0.13**	6.48 ± 0.10##++$$
LVDs, mm	3.23 ± 0.08	3.29 ± 0.11	3.04 ± 0.12	3.24 ± 0.12	3.22 ± 0.07
IVS, mm	2.03 ± 0.12	3.21 ± 0.06**	2.70 ± 0.12**#	2.93 ± 0.13**	1.98 ± 0.12##$$
PW, mm	1.95 ± 0.13	3.29 ± 0.11**	2.70 ± 0.15**#	2.93 ± 0.13**	2.03 ± 0.10##$$
FS, %	49.91 ± 1.09	38.95 ± 2.49**	48.35 ± 1.67##	42.57 ± 2.25*	50.22 ± 1.23##$
E/A ratio	2.04 ± 0.18	1.24 ± 0.14**	1.71 ± 0.08	1.47 ± 0.11**	2.12 ± 0.12##$

NS, normal salt diet; HS, high salt diet; RHT, repetitive hyperthermia; BW, body weight; HW, heart weight; BP, blood pressure; HR, heart rate; bpm, beats/min; LVEDP, left ventricular end-diastolic pressure; LVDd, diastolic dimension of left ventricle; LVDs, systolic dimension of left ventricle; IVS, thickness of interventricular septum; PW, thickness of posterior wall; FS, ratio of left ventricular fractional shortening; E/A ratio, peak velocity of early transmitral inflow (E)-to-peak velocity of late transmitral inflow (A) ratio. *$P < 0.05$ vs. NS, **$P < 0.01$ vs. NS, #$P < 0.05$ vs. HS, ##$P < 0.01$ vs. HS, +$P < 0.05$ vs. HS+RHT, ++$P < 0.01$ vs. HS+RHT, \$$P < 0.05$ vs. HS+RHT +17-DMAG, \$\$$P < 0.01$ vs. HS+RHT +17-DMAG.

HS+RHT+17-DMAG groups, the thicknesses of IVS and PW were significantly increased, and LVDd, LVDs, and FS were reduced at 10 wk of age compared with the values in the NS group (Table 1). However, in the HS+RHT group, the wall thicknesses of the IVS and PW were significantly reduced, and LVDd and FS were increased compared with the values in the HS group. In addition, the E/A ratio was significantly decreased in the HS group at 10 wk of age, compared with that in the NS group, and this decrease was significantly less in the HS+RHT group. To elucidate the BP-lowering effects of RHT on cardiac morphology and function by hyperthermia, the DS rats receiving HS diet were administered hydralazine for 4 wk (HS+Hy; Supplemental Data). Although BP was similar between HS+RHT and HS+Hy groups, cardiac hypertrophy, including thicker IVS and PW, and reduced cardiac function, including FS and E/A ratio, were recognized in HS+Hy group compared with those in HS+RHT group. (Supplemental Table and Figure).

Histology. Figure 2*B* shows representative histological specimens of myocardial sections demonstrating changes in cell

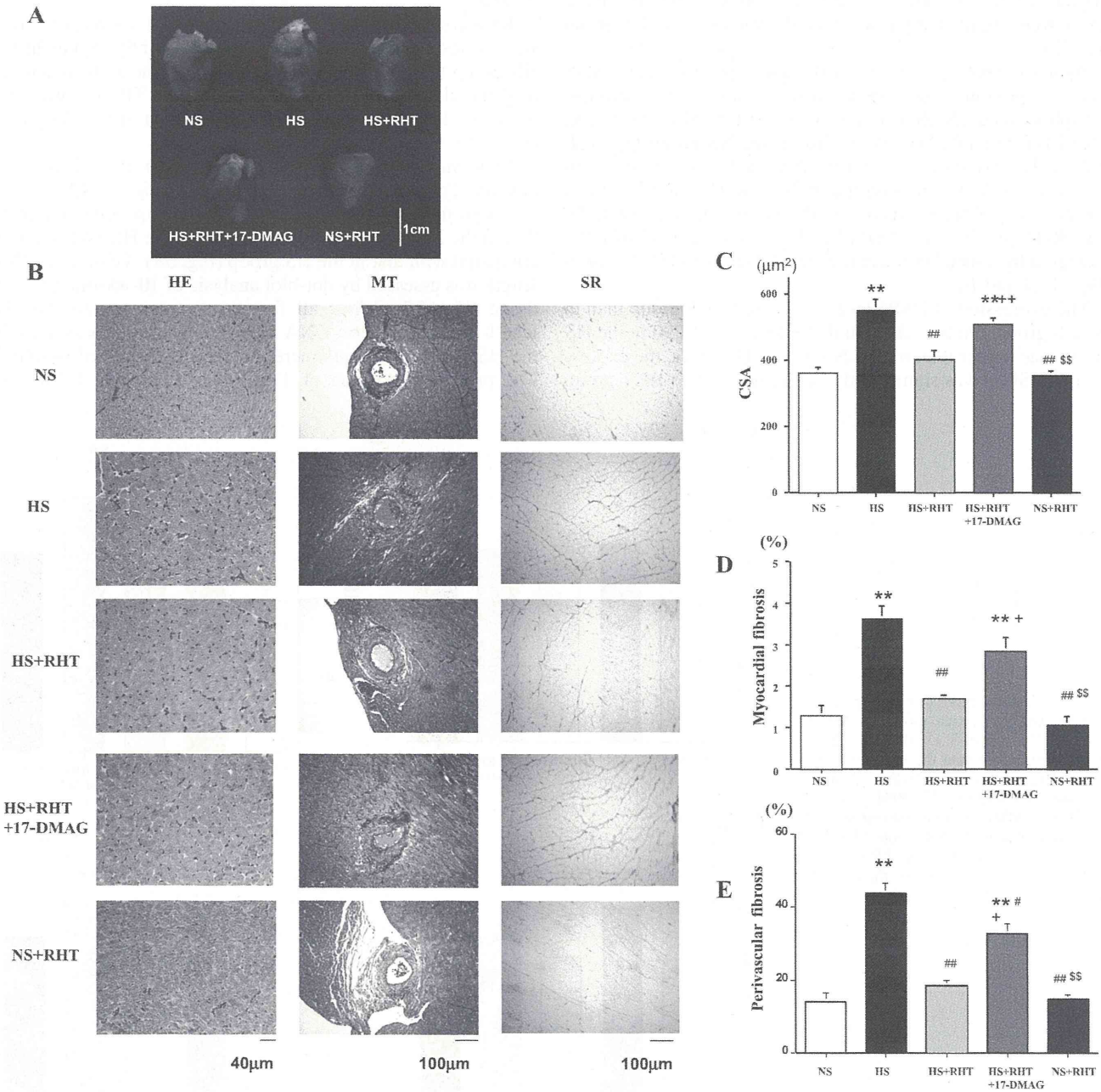

Fig. 2. *A*: representative photos of the hearts in each of the 5 groups. *B*: representative histological examination by hematoxylin-eosin (HE) staining (*left* lane), Masson's trichrome (MT) staining (*middle* lane), Sirius red staining (*right* lane) in each group at 10 wk of age. Cross-sectional area (CSA) of cardiomyocytes (*C*), myocardial interstitial fibrosis (*D*), and perivascular fibrosis (*E*) in each group. $^{**}P < 0.01$ vs. the NS group. $\#P < 0.05$, $\#\#P < 0.01$ vs. the HS group. $+P < 0.05$, $++P < 0.01$ vs. the HS+RHT group. $\$\$P < 0.01$ vs. the HS+RHT+17-DMAG group.

size and vascular structure at 10 wk of age in each group. The cardiomyocyte CSA was significantly larger in the HS group than in the NS group; however, hyperthermia significantly ameliorated CSA in the HS+RHT group compared with the HS group (Fig. 2*C*). The degree of myocardial interstitial or perivascular fibrosis was increased by an HS diet, but was attenuated by hyperthermia (Fig. 2, *D* and *E*).

Myocardial MMP activities. Myocardial activities of MMP-1, -2, -3, -9 in the HS group were elevated compared with the values in the NS group. However, RHT suppressed the enzymatic increases in MMP-2, -3, -9 due to salt-induced hypertrophic cardiac remodeling since the values in the HS+RHT group were significantly lower than the values in the HS group (Fig. 3).

Western blotting analysis. Although expressions of eNOS and Akt proteins were comparable among the five groups, phosphorylated eNOS was lower in the HS, HS+RHT, and HS+RHT+17-DMAG groups than in the NS group(Fig. 4, *B* and *C*). The expression of phosphorylated Akt in the HS group was reduced compared with that in NS and HS+RHT groups; however, hyperthermia increased the expression of pAkt in the HS+RHT group, and 17-DMAG decreased the level of pAkt increased by hyperthermia in the HS+RHT+17-DMAG group (Fig. 4, *D* and *E*).

The expression of HSP60 was lower in the HS group than in the NS group. On the other hand, the level of HSP90 in the HS group was higher than that in NS group. However, the expression of HSP60 was significantly higher in the HS+RHT group than in the HS group, and the expressions of HSP70 and 90 were significantly higher in the HS+RHT and HS+RHT+17-DMAG groups than in both the HS and NS groups (Fig. 4, *F–H*). In the NS+RHT group, all HSPs increased compared with those in the NS group.

The expressions of TLR-4, iNOS, nitrotyrosine, PTX3, and BNP increased in the HS group compared with those in the NS and HS+RHT groups. However, RHT inhibited the increase, since the expressions in the HS+RHT group were significantly lower than those in the HS group (Fig. 4, *I–M*). 17-DMAG partially attenuated the effects of RHT on myocardial inflammation.

Myocardial oxidative stress. Myocardial oxidative stress was expressed as TBARS and was significantly higher in the HS group than in the NS group. However, heat stress attenuated the elevation of oxidative stress since TBARS was significantly lower in the HS+RHT group than in the HS group (Fig. 4*N*).

Hyperthermia preserved telomere length and telomerase activity. Telomerase activity, quantified using a TRAP assay, was significantly decreased in the HS group compared with that in the NS group but was increased in the HS+RHT group compared with that in the HS group (Fig. 5*A*). Telomeric DNA length was assessed by dot-blot analysis of 10-wk-old rat heart tissue (Fig. 5*B*). When all five groups were compared, the length of the telomeric DNA was significantly shorter only in the HS group. Thus, telomere length was preserved by RHT. The protein expression of TERT was attenuated in the HS

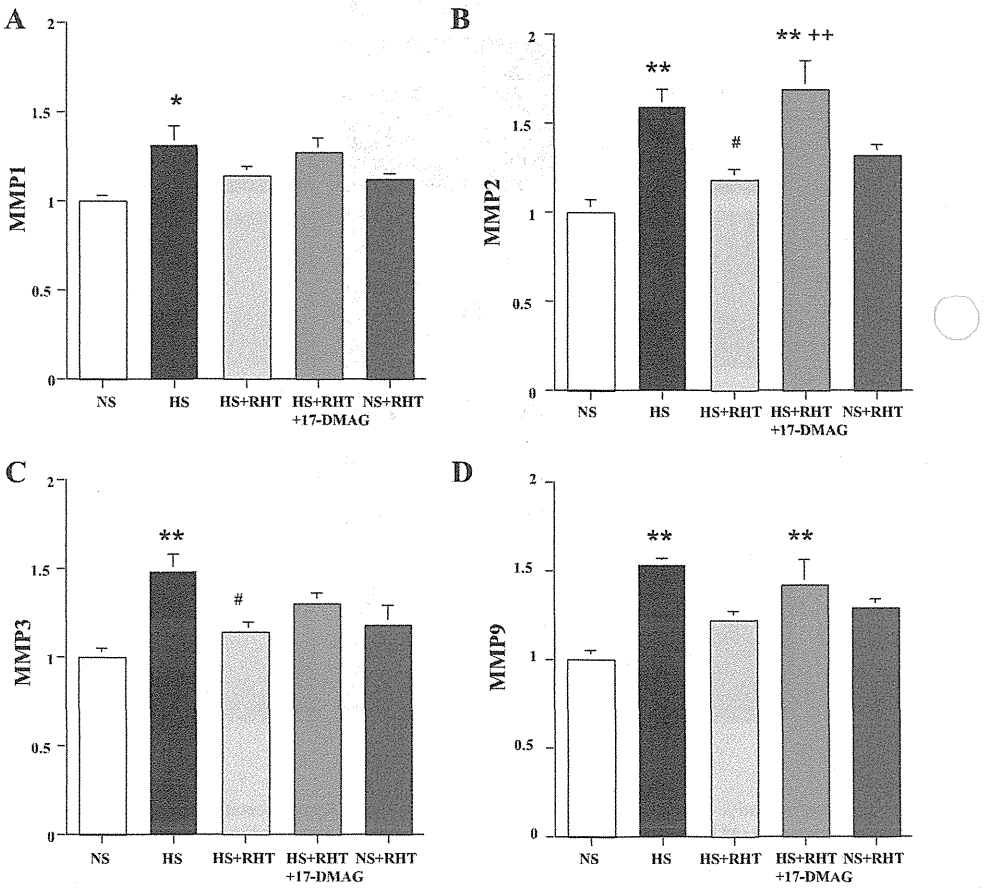

Fig. 3. Cardiac matrix metalloproteinase (MMP) activity in each group. *A*: MMP-1, *B*: MMP-2, *C*: MMP-3, *D*: MMP-9 in the HS group were higher than the levels in the NS group. The increases in MMP-2, -3, and -6 were suppressed in the HS+RHT group. The activities of MMPs were expressed as a relative ratio to that in the NS group. $*P < 0.05$, $**P < 0.01$ vs. the NS group. $\#P < 0.05$ vs. the HS group. $++P < 0.01$ vs. the HS+RHT group.

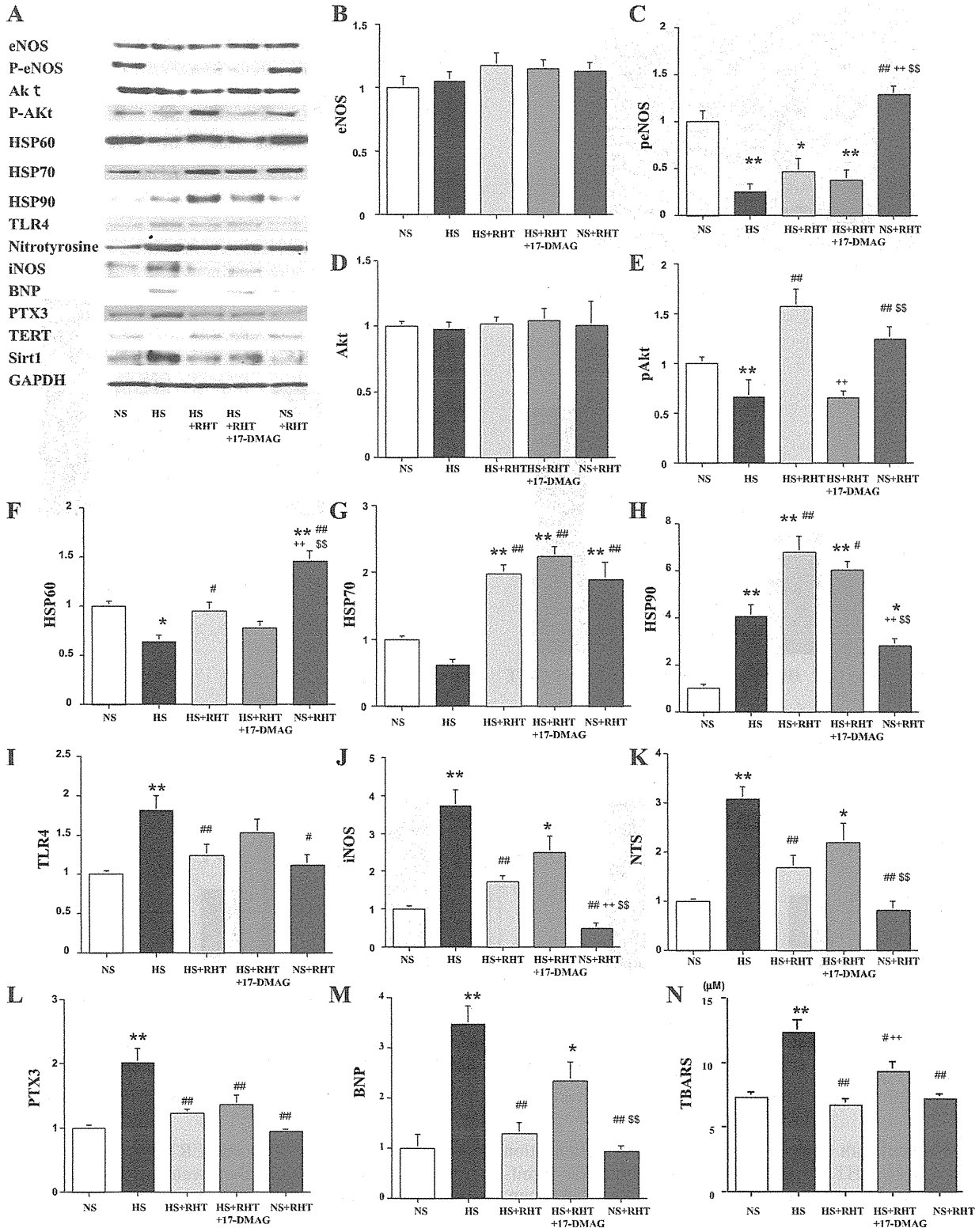

Fig. 4. Analysis of protein expression by Western blotting or ELISA assay in the hearts in each group. Representative data and summarized results (*A*) for endothelial nitric oxide synthase (eNOS, *B*), phosphor-eNOS (*C*), Akt (*D*), phosphor-Akt (*E*), heat shock protein (HSP) 60 (*F*), HSP70 (*G*), HSP90 (*H*), Toll-like receptor (TLR)-4 (*I*), iNOS (*J*), nitrotyrosine (NTS) (*K*), pentraxin (PTX) 3 (*L*), brain natriuretic peptide (*M*), thiobarbituric acid reactive substances (TBARS, *N*). The expression of GAPDH was used as an internal control. The average density value of each protein was expressed as a relative ratio to that in the NS group normalized by GAPDH (*B–M*). The levels of myocardial TBARS are expressed in *N*. $*P < 0.05$, $**P < 0.01$ vs. the NS group. $\#P < 0.05$, $\#\#P < 0.01$ vs. the HS group. $+P < 0.01$ vs. the HS+RHT group. $\$\$P < 0.01$ vs. the HS+RHT+17-DMAG group.

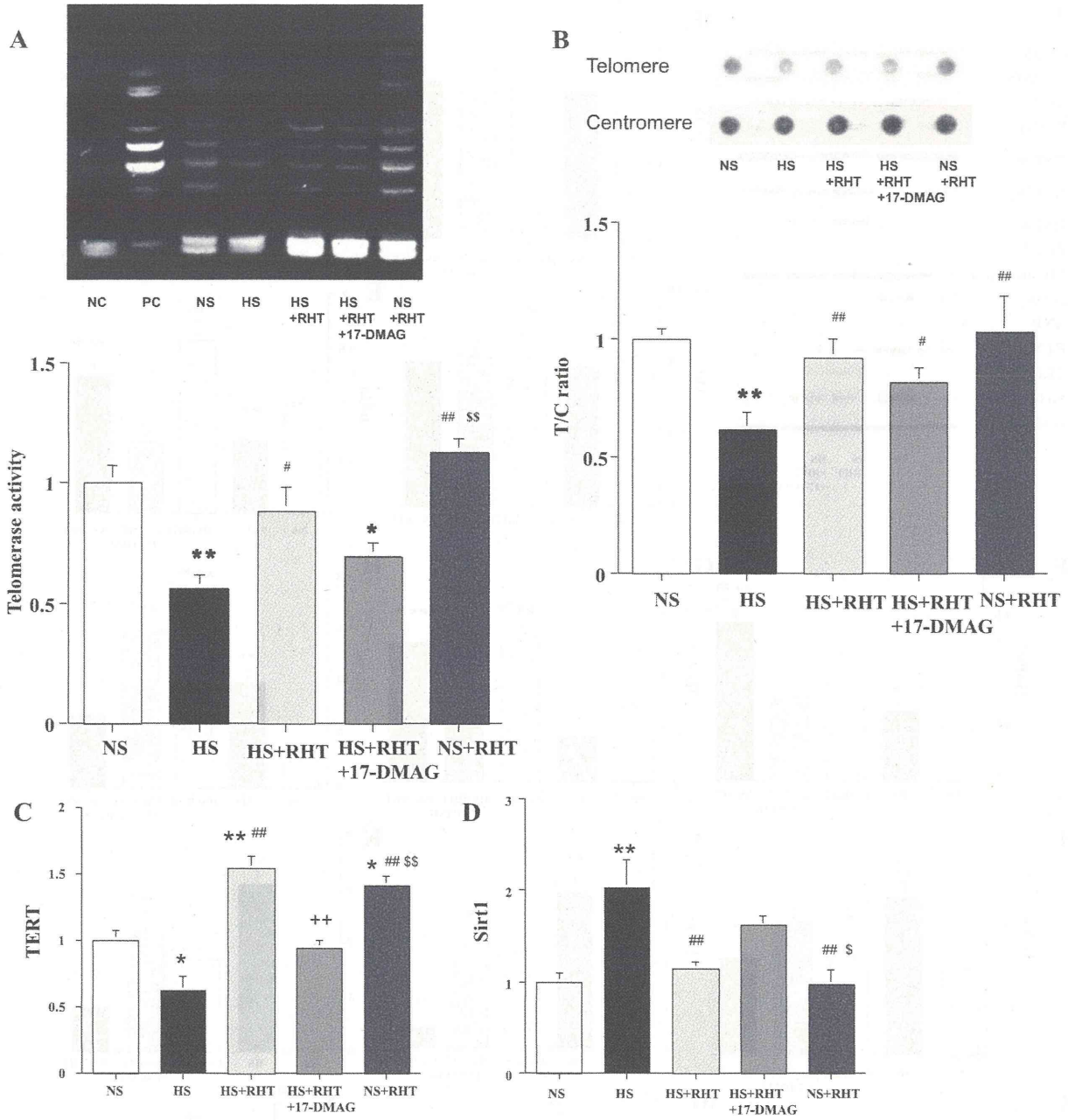

Fig. 5. Telomerase activity in the hearts in each group. Telomerase activity was normalized by that in the NS group (*A*). PC, positive control; NC, negative control. The length of telomeric DNA in the heart, as assessed by dot-blot analysis, is presented as the telomeric-to-centromeric DNA content (T/C) ratio, which was normalized by that in the NS group (*B*). The protein levels for telomere reverse transcriptase (TERT) and Sirt1 in the heart were determined by Western blot analysis (*C, D*). The expressions of proteins are expressed as a relative ratio to that in the NS group normalized by GAPDH. $*P < 0.05$, $**P < 0.01$ vs. the NS group. $\#P < 0.05$, $\#\#P < 0.01$ vs. the HS group. $+P < 0.01$ vs. the HS+RHT group. $\$P < 0.05$, $\$\$P < 0.01$ vs. the HS+RHT+17-DMAG group.

group compared with that in the NS group, but this attenuation was reversed by RHT. Although the level of Sirt1 was significantly increased in the HS group compared with the NS group, this increase was not observed in the HS+RHT group (Fig. 5, *C* and *D*).

DISCUSSION

The novel findings of this study are that salt-induced cardiac hypertrophy causes increased cardiac inflammation, shortening of telomere length, and reduced TERT and telomerase activity. Furthermore, RHT prevents the development of cardiac remodeling, suppresses cardiac inflammation and oxidative stress, and preserves telomere length. To the best of our knowledge, this is the first study that shows RHT attenuates the progression of cardiac hypertrophy, which can lead to DHF.

Hyperthermia, cardiac hypertrophy, and ventricular function. Warm water immersion increases cardiac output and stroke volume and decreases systemic vascular resistance (18, 35).

Tei and coworkers (11, 13, 14) demonstrated that RHT using dry sauna increases eNOS protein in hamsters with CHF and improves cardiac dysfunction in patients with heart failure. Therefore, a reduction in cardiac afterload by hyperthermia may contribute to the prevention of hypertrophy. In the present study, when DS rats fed an HS diet were subjected to brief daily episodes of mild hyperthermia, the increase in BP and cardiac hypertrophy were attenuated. However, when mice fed an HS diet were received hydralazine to adjust similar BP to that in HS+RHT group, all of the preventive changes that were seen in the HS+RHT group including cardiac hypertrophy and protein expression compared with the HS group could not be inhibited only by BP adjustment. Therefore, the treatment with RHT may perform the cardioprotective effects beyond BP control. In the NS+RHT group, RHT increased HSPs with decreasing myocardial inflammation. Although the additional effects on normal cardiac function and remodeling were recognized apparently, RHT attenuated the changes in ventricular function that can lead to CHF, such as an increase in LVEDP, reduction in FS, and reduction in E/A ratio against the burden of an HS diet and developing cardiac hypertrophy beyond the reduction in BP by hyperthermia.

MMP activity. Cardiac remodeling results from an imbalance between the synthesis and degradation of extracellular matrix proteins and plays a key role in the pathophysiology of heart failure (12). Therefore, MMPs are essential in extracellular matrix degradation (19). In the failing heart, there are increased levels of MMPs, including -2, -3, and -9 (32, 33). Furthermore, the activation of MMP-2 was found to accompany progressive myocardial fibrosis, and MMP-9 was activated in rat heart failure (20, 27). Our data suggested that MMP-1,-2,-3, and -9 were all increased by salt-induced hypertension. However, RHT attenuated the activation of MMPs, which may be involved in the improvement of cardiac remodeling.

HSP. HSP70 and 72 have cytoprotective properties against ischemia/reperfusion injury in vitro and in vivo (12, 22), and HSP90 upregulates eNOS activity in vivo (25, 30).

In pacing-induced CHF in dogs, the levels of HSP60 and 70 rapidly increased by 24 h after pacing, although HSP90 was still low. On the other hand, induction of HSP90 was overt at 2 wk after pacing despite the restoration of normal levels of HSP60 and 70 (4). In the present study, the protein levels of HSP60 and 70 were only modestly decreased after 4 wk of hypertension, despite a rather dramatic increase in HSP90. Importantly, all three HSPs were significantly increased by RHT. Therefore, HSPs induced by hyperthermia may protect against cardiac injury and oxidative stress. HSP60 and 70 are possible ligands for TLR4 (1, 21). Exogenous HSPs including microbial HSPs as foreign bodies and extracellular HSPs released from injured cell activate TLR4 signaling. However, endogenous HSP induced by heat shock and drug have cardioprotective effects against myocardial injury (12, 22). RHT suppressed myocardial inflammation, which activated TLR4 induction, resulting in decreased expression of TLR4.

In this study, HSP90 is involved in the effects of RHT partially as 17-DMAG diminished the effect of RHT slightly.

Oxidative stress and inflammation. Evidence from experimental models of heart failure show that oxidative stress is increased in the failing heart and contributes to the pathophysiology of heart failure (5). iNOS, oxidative stress, and nitrotyrosine, which is the footprint of peroxynitrite, were induced by inflammation caused by heart failure (23).

TLR-4 expression is upregulated in patients or animal models with cardiac dysfunction (7, 24) and thought to be a toll gate to the various inflammatory responses to immunological stress. In this study, upregulated signaling of TLR-4 was suppressed by RHT.

PTX-3, which is a prototypic member of the long pentraxin family, is structurally related to, but distinct from the classic short pentraxin, C-reactive protein or serum amyloid proteins. PTX3 is produced by a variety of cell types, including monocytes/macrophages, vascular endothelial cells, vascular smooth muscle cells, adipocytes, fibroblasts, and dendritic cells in response to primary inflammatory stimuli (10). The plasma levels of PTX3 are increased in patients with CHF (15).

Our data suggest that elevated TLR4, iNOS, TBARS, nitrotyrosine, PTX3, and BNP in salt-induced hypertension were prevented by RHT. The beneficial effects of hyperthermia might be attributable in part to a reduction in myocardial oxidative stress in addition to a decrease in myocardial inflammation, which resulted in preserved cardiac function.

Telomere biology. The Framingham heart study demonstrates that hypertension, insulin resistance, and oxidative stress are associated with relatively short telomere length in human leukocytes (3). Telomere length was found to vary inversely with age, and age-adjusted telomere length was shorter in individuals with cardiovascular disease than in healthy individuals (9, 29). Shortening of the telomeres has been shown to be associated with an increased rate of mortality from heart disease. The ribonuclear complex telomerase is the central component of the telomere complex. The enzyme complex of telomerase contains a catalytic subunit, TERT. In isolated cells, TERT gene transfer reduces replicative senescence and extends the lifespan of numerous cell types including cardiomyocytes (2). Thus, telomere-associated proteins are thought to be important for the regulation of cardiac muscle cell growth and survival (26). A recent study suggested that moderate overexpression of Sirt1 protects the heart against oxidative stress. The antiaging and stress-resistance effects of Sirt1 may protect the heart from oxidative stress by facilitating the expression of antioxidants (17, 34). In the present study, we found that salt-induced hypertension caused telomere shortening, reduced activity of telomerase, and decreased expression of TERT and that these changes were prevented by RHT. In the present study, telomerase activity was inhibited and downregulated in the HS group compared with that in the NS group. However, RHT led to a recovery of the expression of TERT and preservation of the length of telomeric DNA.

Limitations

There are few limitations of this study. First, systemic BP was reduced by RHT. However, the lowering BP did not improve the cardiac remodeling, function, and protein expressions in the group in which BP was adjusted by hydralazine (HS+Hy) to the extent to that in the HS+RHT group in the supplemental study. As the whole effects of RHT contain not only the slight BP-lowering effect but also a preventive effect of increasing BP probably due to increased eNOS by increased shear stress and HSP, the combined mechanisms of RHT including the above-mentioned prevent cardiac hypertrophy in

Dahl hypertensive rat. Second, Dahl hypertensive rats receiving the HS diet developed cardiac hypertrophy but still preserved cardiac systolic function at the compensated stage in this study. The follow-up period was not enough for CHF to develop, and thus we could not show a beneficial effect of RHT on the development of systolic CHF sufficiently. Further longer observation would be needed. However, it is very likely that hyperthermia would reduce mortality in this experimental model.

In conclusion, RHT attenuates the development of cardiac hypertrophy and fibrosis and preserves telomerase, TERT activity, and the length of telomere DNA in salt-induced hypertensive rats through activation of eNOS and induction of HSPs.

ACKNOWLEDGMENTS

The authors thank Keiko Tsuchida, Sachiyo Taguchi, and Yasuko Ueda for expert technical assistance.

GRANTS

This work was supported in part by a grant-in-aid from the Ministry of Education, Science and Culture of Japan.

DISCLOSURES

No conflicts of interest, financial or otherwise, are declared by the author(s).

AUTHOR CONTRIBUTIONS

Author contributions: J.-i.O. and N.M. conception and design of research; J.-i.O. and M.S. performed experiments; T.M. interpreted results of experiments; Y.H. prepared figures; K.N. edited and revised manuscript; N.M. approved final version of manuscript.

REFERENCES

1. **Asea A, Kraeft SK, Kurt-Jones EA, Stevenson MA, Chen LB, Finberg RW, Koo GC, Calderwood SK.** HSP70 stimulates cytokine production through a CD14-dependant pathway, demonstrating its dual role as a chaperone and cytokine. *Nat Med* 6: 435- 442, 2000.
2. **Danial NN, Korsmeyer SJ.** Cell death: critical control points. *Cell* 116: 205–219, 2004.
3. **Demissie S, Levy D, Benjamin EJ, Cupples LA, Gardner JP, Herbert A, Kimura M, Larson MG, Meigs JB, Keaney JF, Aviv A.** Insulin resistance, oxidative stress, hypertension, and leukocyte telomere length in men from the Framingham heart study. *Aging Cell* 5: 325–330, 2006.
4. **De Souza AI, Cardin S, Wait R, Chung YL, Vijayakumar M, Maguy A, Camm AJ, Nattel S.** Proteomic and metabolomic analysis of atrial profibrillatory remodelling in congestive heart failure. *J Mol Cell Cardiol* 49: 851–863, 2010.
5. **Dhalla NS, Temsah RM, Netticadan T.** Role of oxidative stress in cardiovascular diseases. *J Hypertens* 18: 655–673, 2000.
6. **Emoto N, Raharjo SB, Isaka D, Masuda S, Adiarto S, Jeng AY, Yokoyama M.** Dual ECE/NEP inhibition on cardiac and neurohumoral function during the transition from hypertrophy to heart failure in rats. *Hypertension* 45: 1145–1152, 2005.
7. **Frantz S, Kobzik L, Kim YD, Fukazawa R, Medzhitov R, Lee RT, Kelly RA.** Toll4 (TLR4) expression in cardiac myocytes in normal and failing myocardium. *J Clin Invest* 104: 271–280, 1999.
8. **Fukui S, Fukumoto Y, Suzuki J, Saji K, Nawata J, Shinozaki T, Kagaya Y, Watanabe J, Shimokawa H.** Diabetes mellitus accelerates left ventricular diastolic dysfunction through activation of the renin-angiotensin system in hypertensive rats. *Hypertens Res* 32: 472–480, 2009.
9. **Fuster JJ, Andre's V.** Telomere biology and cardiovascular disease. *Circ Res* 99: 1167–1180, 2006.
10. **Garlanda C, Bottazzi B, Bastone A, Mantovani A.** Pentraxins at the crossroads between innate immunity, inflammation, matrix deposition, and female fertility. *Annu Rev Immunol* 23: 337–366, 2005.
11. **Ikeda Y, Biro S, Kamogawa Y, Yoshifuku S, Eto H, Orihara K, Yu B, Kihara T, Miyata M, Hamasaki S, Otsuji Y, Minagoe S, Tei C.** Repeated sauna therapy increases arterial endothelial nitric oxide synthase expression and nitric oxide production in cardiomyopathic hamsters. *Circ J* 69: 722–729, 2005.
12. **Kawana K, Miyamoto Y, Tanonaka K, Han-no Y, Yoshida H, Takahashi M, Takeo S.** Cytoprotective mechanism of heat shock protein 70 against hypoxia/reoxygenation injury. *J Mol Cell Cardiol* 32: 2229–2237, 2000.
13. **Kihara T, Biro S, Imamura M, Yoshifuku S, Takasaki K, Ikeda Y, Otuji Y, Minagoe S, Toyama Y, Tei C.** Repeated sauna treatment improves vascular endothelial and cardiac function in patients with chronic heart failure. *J Am Coll Cardiol* 39: 754–759, 2002.
14. **Kisanuki A, Daitoku S, Kihara T, Otsuji Y, Tei C.** Thermal therapy improves left ventricular diastolic function in patients with congestive heart failure: a tissue doppler echocardiographic study. *J Cardiol* 49: 187–191, 2007.
15. **Kotooka N, Inoue T, Aoki S, Anan M, Komoda H, Node K.** Prognostic value of pentraxin 3 in patients with chronic heart failure. *Int J Cardiol* 130: 19–22, 2008.
16. **Makino N, Maeda T, Oyama J, Higuchi Y, Mimori K.** Improving insulin sensitivity via activation of PPAR-gamma increases telomerase activity in the heart of OLETF rats. *Am J Physiol Heart Circ Physiol* 297: H2188–H2195, 2009.
17. **Makino N, Maeda T, Oyama JI, Sasaki M, Higuchi Y, Mimori K, Shimizu T.** Antioxidant therapy attenuates myocardial telomerase activity reduction in superoxide dismutase-deficient mice. *J Mol Cell Cardiol* 50: 670–677, 2010.
18. **Massett MP, Lewis SJ, Kregel KC.** Effect of heating on the hemodynamic responses to vasoactive agents. *Am J Physiol Regul Integr Comp Physiol* 275: R844–R853, 1998.
19. **Nagase H, Woessner JF Jr.** Matrix metalloproteinases. *J Biol Chem* 274: 21491–21494, 1999.
20. **Nishikawa N, Yamamoto K, Sakata Y, Mano T, Yoshida J, Miwa T, Takeda H, Hori M, Masuyama T.** Differential activation of matrix metalloproteinases in heart failure with, and without ventricular dilatation. *Cardiovasc Res* 57: 766–774, 2003.
21. **Ohashi K, Burkart V, Flohe S, Kolb H.** Heat shock protein 60 Is a putative endogenous ligand of the Toll-Like receptor-4 complex. *J Immunol* 164: 558–561, 2000.
22. **Ooie T, Takahashi N, Saikawa T, Nawata T, Arikawa M, Yamanaka K, Hara M, Shimada T, Sakata T.** Single oral dose of geranylgeranylacetone induces heat-shock protein 72 and renders protection against ischemia/reperfusion injury in rat heart. *Circulation* 104: 1837–1843, 2001.
23. **Oyama J, Shimokawa H, Momii H, Cheng X, Fukuyama N, Arai Y, Egashira K, Nakazawa H, Takeshita A.** Role of nitric oxide and peroxynitrite in the cytokine-induced sustained myocardial dysfunction in dogs in vivo. *J Clin Invest* 101: 2207–2214, 1998.
24. **Oyama J, Blais C Jr, Liu X, Pu M, Kobzik L, Kelly RA, Bourcier T.** Reduced myocardial ischemia-reperfusion injury in toll-like receptor 4-deficient mice. *Circulation* 109: 784–789, 2004.
25. **Pritchard KA Jr, Ackerman AW, Gross ER, Stepp DW, Shi Y, Fontana JT, Baker JE, Sessa WC.** Heat shock protein 90 mediates the balance of nitric oxide and superoxide anion from endothelial nitric-oxide synthase. *J Biol Chem* 276: 17621–17624, 2001.
26. **Prowse KR, Greider CW.** Developmental and tissue-specific regulation of mouse telomerase and telomere length. *Proc Natl Acad Sci USA* 92: 4818–4822, 1995.
27. **Sakata Y, Yamamoto K, Mano T, Nishikawa N, Yoshida J, Hori M, Miwa T, Masuyama T.** Activation of matrix metalloproteinases precedes left ventricular remodeling in hypertensive heart failure rats: its inhibition as a primary effect of Angiotensin-converting enzyme inhibitor. *Circulation* 109: 2143–2149, 2004.
28. **Senni M, Tribouilloy CM, Rodeheffer RJ, Jacobsen SJ, Evans JM, Bailey KR, Redfield MM.** Congestive heart failure in the community: a study of all incident cases in Olmsted County, Minnesota, in 1991. *Circulation* 98: 2282–2289, 1991.
29. **Serrano AL, Andres V.** Telomeres and cardiovascular disease. Does size matter? *Circ Res* 94: 575–584, 2004.
30. **Shi Y, Baker JE, Zhang C, Tweddell JS, Su J, Pritchard KA Jr.** Chronic hypoxia increases endothelial nitric oxide synthase generation of nitric oxide by increasing heat shock protein 90 association and serine phosphorylation. *Circ Res* 91: 300–306, 2002.

31. **Shiomi T, Tsutsui H, Matsusaka H, Murakami K, Hayashidani S, Ikeuchi M, Wen J, Kubota T, Utsumi H, Takeshita A.** Overexpression of glutathione peroxidase prevents left ventricular remodeling and failure after myocardial infarction in mice. *Circulation* 109: 544–549, 2004.
32. **Spinale FG, Coker ML, Heung LJ, Bond BR, Gunasinghe HR, Etoh T, Goldberg AT, Zellner JL, Crumbley AJ.** A matrix metalloproteinase induction/activation system exists in the human left ventricular myocardium and is upregulated in heart failure. *Circulation* 102: 1944–1949, 2000.
33. **Spinale FG, Coker ML, Bond BR, Zellner JL.** Myocardial matrix degradation and metalloproteinase activation in the failing heart: a potential therapeutic target. *Cardiovasc Res* 46: 225–238, 2000.
34. **Tanno M, Kuno A, Yano T, Miura T, Hisahara S, Ishikawa S, Shimamoto K, Horio Y.** Induction of manganese superoxide dismutase by nuclear translocation and activation of SIRT1 promotes cell survival in chronic heart failure. *J Biol Chem* 285: 8375–8382, 2010.
35. **Tei C, Horikiri Y, Park JC, Jeong JW, Chang KS, Toyama Y, Tanaka N.** Acute hemodynamic improvement by thermal vasodilation in congestive heart failure. *Circulation* 91: 2582–2590, 1995.
36. **Vasan RS, Larson MG, Benjamin EJ, Evans JC, Reiss CK, Levy D.** Congestive heart failure in subjects with normal versus reduced left ventricular ejection fraction: prevalence and mortality in a population-based cohort. *J Am Coll Cardiol* 33: 1948–1955, 1999.

The gender-related alterations in the telomere length and subtelomeric methylation status in patients with Parkinson's disease

Toyoki Maeda,[1] Jing-Zhi Guan,[2] Masamichi Koyanagi,[1] Naoki Makino[1]

[1]Department of Cardiovascular, Respiratory and Geriatric Medicine, Kyushu University Beppu Hospital, Japan; [2]The 309th Hospital of Chinese People's Liberation Army, Beijing, China

Abstract

The aim of this study was to determine whether Parkinson's disease affects somatic telomeric features. Some recent reports have shown that telomere length is not changed in patients with Parkinson's disease (PD). In this study, we more closely evaluated possible Parkinson's disease-associated telomeric alterations than has been done previously. We analyzed the telomere length distribution, the subtelomeric methylation status, and their gender-related differences, as well as the mean telomere length in PD patients in comparison to age-matched controls. The telomeric parameters of the peripheral leukocytes of Parkinson's disease outpatients and normal healthy volunteers, including family members of the participating outpatients were determined by analyzing the densitometries of the Southern blot results obtained with methylation-sensitive and insensitive isoschizomers. The Parkinson's patients had gender related-differences in the alterations of their telomere length and subtelomeric status. Only female patients had significant Parkinson's disease-associated telomeric and subtelomeric changes. The female Parkinson's patients bore proportionally decreased long telomeres (>9.4 Kb) and less methylation of short telomeres (<4.4 Kb) in comparison with healthy controls, both of which have been regarded to be a part of aging-associated telomeric and subtelomeric changes. These results suggested that the aging-related telomeric and subtelomeric changes are accelerated specifically in female Parkinson's patients, and that genomic DNA is more strongly affected by Parkinson's disease in females than in males.

Introduction

A telomere is a structure consisting of thousands of hexamer (TTAGGG/AATCCC) repeats and accessory peptide factors located at the termini of human chromosomes.[1,2] Telomeres become shortened little by little because of the inability of complete DNA duplication at the chromosome ends. This process is known as the *end-replication problem*. Such telomere shortening has been observed in peripheral blood nuclear cells with aging in a gender-related manner.[3] In addition, telomere shortening is accelerated by various pathological conditions including physical and mental stress, which yield systemic or local oxidative stress. In fact, telomere shortening is accelerated by disease conditions such as mental stress, obesity, smoking, type 2 diabetes mellitus, ischemic heart diseases, Alzheimer's disease, and sarcoidosis.[4-9] In all of these reported diseases, increased oxidative stress has been suggested to potentially relate to the enhanced shortening of telomere. Such pathophysiological conditions can be hypothesized to affect not only the telomeric structure itself but also the surrounding genomic structures including the epigenetic status, such as DNA methylation. Shortened telomeres have been reported to tend to accompany subtelomeric hypomethylation in mice of fifth generation the telomerase activity-deficient *tert-/tert-* mutant mouse.[10] Therefore, aging-associated telomere length shortening may also be affected by less methylation in the subtelomeric region. The subtelomeric methylation status can be associated with aging-related telomere attrition, which is enhanced in various kinds of disease conditions. Parkinson's disease (PD) is a neurodegenerative disorder characterized by a progressive degeneration of dopaminergic neurons. Localized chronic inflammation and mitochondrial dysfunction are the causative factors of pathogenetical oxidative stress for neurodegeneration in PD.[11-15] Restricted motor behavior enhances mental stress of PD patients. The causative and the secondary stress for PD may cause fragility in the telomeric and subtelomeric structure of circulating leukocytes. It has been hypothesized that the elevated oxygen stress associated with PD may lead to telomere shortening. Some reports, however, have shown that the somatic telomere length is not shorter in PD patients.[16-18] We herein tried to confirm whether or not the telomere structure is altered in PD patients. In order to detect the detailed aging-related changes in the telomeric structure in PD patients, the subtelomeric methylation changes associated with aging as well as the telomere length changes were analyzed in healthy Japanese subjects and Japanese PD patients.

Correspondence: Toyoki Maeda, Department of Cardiovascular, Respiratory and Geriatric Medicine, Kyushu University Beppu Hospital, 4546 Tsurumihara, Beppu, Oita 874-0838, Japan.
E-mail: maedat@beppu.kyushu-u.ac.jp

Key words: Parkinson's disease, DNA methylation, subtelomere, telomere, gender.

Acknowledgments: this work was supported, in part, by a Grant-in-Aid from the Ministry of Education, Science, and Culture of Japan (#23590885) and the National Natural Science Fund (NSFC) (81170329/H2501). We thank Ms. Ueda and Ms. Taguchi for their valuable technical assistance.

Conflict of interests: the authors report no potential conflict of interests.

Received for publication: 27 September 2011.
Revision received: 19 January 2012.
Accepted for publication: 16 May 2012.

Ageing Research 2012; 4:e9
doi:10.4081/ar.2012.e9

Materials and Methods

Study population

Parkinson's disease patients (19 men and 17 women) visiting the outpatient clinic of the Kyushu University Beppu Hospital from November 2008 through December 2010 were enrolled, and some of their family members and some of our hospital's healthy workers, who passed a regular medical check-up within a year before the enrollment, were also enrolled as healthy controls (27 men and 22 women). The present research was performed, following the approval by the Conjoint Health Research Ethics Board of Kyushu University, and written consent was obtained from all the participants. DNA samples were obtained from peripheral leukocytes of *de novo* female PD patients diagnosed according to the Japan Parkinson's Disease Society Brain Bank criteria. Blood samples were collected from the patients before the administration of anti-Parkinson agents started. The numbers and the ages of the participants are described in Table 1. There were no statistical differences in the ages between males and females, and between controls and PD patients. Blood samples were drawn, using heparinized syringes and 10 mL vacutainer

tubes. We added over 20 times the volume of 10 mm Tris-HCl, 1 mm EDTA (pH 8.0) to the blood sample to remove erythrocytes by lowering osmotic pressure. Next, peripheral leukocytes were collected by centrifugation.

Telomere detection

Telomere detection was performed as previously described with a modification (3). Methylation-sensitive and -insensitive isoschizomers, *Hpa*II and *Msp*I, were used. Briefly, blood cell DNA was extracted from samples and the DNA (1 μg) were digested. The digests (10 μL) were Southern hybridized to a probe of 500 bp long (TTAGGG)n labeled with digoxigenin (dig). The smears of the autoradiogram were captured on an Image Master, and the telomere length was then assessed quantitatively. Every sample was measured in triplicate.

Terminal restriction fragment length analysis

The mean terminal *Msp*I-restriction fragment lengths (TRFs) were estimated using the formula Σ(ODi-background)/Σ(ODi-background/Li), where ODi is the densitometric intensity and Li is the length of the TRF fragment at position i. Telomere length distribution was analyzed by comparing the telomere length using a telomere percentage analysis with three intervals of length as defined by a molecular weight standard as previously described.[3,9] The Southern blot smear intensity was quantified as follows: each telomeric sample was divided into grid squares as follows according to the molecular size ranges: >9.4, 9.4> >4.4 and 4.4 >Kb. The percent of the divided intensity in each molecular weight range was measured (intensity of a defined region-background×100/total lane intensity-background). Subtelomeric methylation was assessed by comparing *Msp*I-TRF and *Hpa*II-TRF (H-M TRF) and by comparing *Msp*I telomere length distribution and *Hpa*II telomere length distribution. Subtelomeric methylation status of size-fractioned telomeres was analyzed to know the extents of subtelomeric methylation with different telomere sizes. The difference between the percent of *Msp*I signal intensity (%*Msp*I-TRF) and the *Hpa*II signal intensity (%*Hpa*II-TRF) in each molecular weight range was calculated. The proportion of the calculated difference (%*Hpa*II-TRF %*Msp*I-TRF) in >9.4 Kb range to %*Hpa*II-TRF in >9.4 Kb range was used to evaluate the methylation status of telomeres with telomeric and subtelomeric methylated region longer than 9.4 Kb. Similarly, the proportion of the calculated difference (%*Msp*I-TRF %*Hpa*II-TRF) in <4.4 Kb range to %*Msp*I-TRF in >4.4 Kb range was used to evaluate the methylation status of telomeres shorter than 4.4 Kb.

Statistical analysis

The normality of the data was examined with the Kolmogorov-Smirnov test and the homogeneity of variance with the Levene Median test. If both the normal distribution and equal variance tests were passed, the differences in the telomeres length including the mean TRF length and the telomere percentage analysis with age and condition (AD patients or age-matched healthy controls) were studied using a two-way analysis of variance (ANOVA) test followed by all pairwise multiple comparison procedures using Tukey's post hoc test. The data are expressed as the mean+standard deviation. The criterion for the significance is $P<0.05$. All analyses were carried out using a Sigma Statistical Analysis software package (Sigma 2.03, 2001; St. Louis, MO).

Results

The PD patients showed no significant changes in the *Msp*I-TRF in comparison to con-

Table 1. The ages of the participants

		Normal (n)	Parkinson (n)	P-value (disease-related)
Males				
	Age	54.3±4.6 (27)	56.0±4.4 (19)	0.21
	Age range	49-64	49-62	
Females				
	Age	55.0±4.6 (22)	57.4±4.4 (17)	0.12
	Age range	48-62	47-61	
P-value (gender-related)		0.57	0.36	-

Age: the mean value±standard deviation in years. n: the numbers of the participants.

Table 2. The telomeric parameters of the participants

						P-value		
	PM	PF	NM	NF	PM/NM	PF/NF	PM/PF	NM/NF
*Msp*I-TRF (Kb)	6.9±0.9	6.6±1.2	6.6±1.3	7.4±1.5	0.350	0.083	0.341	0.079
*Hpa*II-TRF (Kb)	8.2±1.0	7.8±1.2	7.9±1.3	8.8±1.5	0.349	0.029	0.288	0.031
H-M-TRF (Kb)	1.3±0.5	1.2±0.6	1.3±0.5	1.4±0.5	0.941	0.208	0.745	0.223
>9.4 Kb *Msp*I (%)	33.3±11.6	29.6±12.2	31.0±12.0	38.3±13.6	0.523	0.043	0.353	0.058
9.4-4.4 Kb *Msp*I (%)	56.3±8.3	56.4±7.1	55.4±8.5	51.6±6.7	0.736	0.043	0.978	0.088
<4.4 Kb *Msp*I (%)	10.4±5.6	14.1±7.6	13.5±8.0	10.1±8.8	0.133	0.140	0.113	0.172
>9.4 Kb *Hpa*II(%)	48.4±10.7	45.9±12.4	45.2±10.8	54.9±13.0	0.332	0.035	0.526	0.008
9.4-4.4 Kb *Hpa*II (%)	47.9±9.2	48.7±9.6	50.4±9.0	41.9±9.9	0.362	0.038	0.796	0.003
<4.4 Kb *Hpa*II (%)	3.8±3.4	5.4±3.5	4.4±3.3	3.2±3.9	0.521	0.066	0.157	0.243
>9.4 Kb H-M (%)	15.1±6.1	16.3±6.6	14.2±6.5	16.6±6.5	0.635	0.893	0.562	0.197
<4.4 Kb H-M (%)	-6.6±3.5	-8.6±4.9	-9.1±5.6	-6.9±5.5	0.078	0.31	0.176	0.182
H-M/H >9.4 Kb	0.32±0.13	0.37±0.15	0.32±0.15	0.31±0.13	0.100	0.232	0.318	0.841
M-H/M <4.4 Kb	0.67±0.18	0.58±0.20	0.70±0.17	0.75±0.14	0.594	0.006	0.181	0.202

NM, normal males; NF normal females; PM Parkinson's males; PF Parkinson's females.

trols in both genders (Table 2, Figure 1). On the other hand, the *Hpa*II-TRF was shorter in female PD patients, indicating that the methylated terminal fragment length can be affected in a gender-specific manner. However, the subtracted *Hpa*II-*Msp*I TRFs were not significantly different between controls and PD patients. Therefore, the mean length range of the methylated subtelomeres did not seem to be changed in PD patients. In the proportional telomere length distribution, the long TRFs (>9.4 Kb), *Msp*I-TRF and *Hpa*II-TRF, decreased, and the intermediate TRFs (9.4-4.4 Kb) increased specifically in female PD patients (Table 2, Figure 2). This indicated that the proportional amount of long *Msp*I-TRF (>9.4 Kb) was a more sensitive measure to detect the telomeric length change than the mean *Msp*I-TRF. The subtracted distribution, the *Hpa*II-TRF distribution minus the *Msp*I-TRF distribution, was not statistically different between controls and PD patients (Table 2, Figures 3, 4). Moreover, we tried to analyze the *Msp*I- and *Hpa*II-TRF distribution by comparing the proportions between the %*Msp*I-TRF and %*Hpa*II-TRF in the size ranges in order to detect relative subtelomeric methyaltion status without the bias associated with the absolute percentages of *Msp*I-TRF or *Hpa*II-TRF. For this purpose, we used (%*Msp*I-TRF - %*Hpa*II-TRF)/%*Msp*I-TRF for the TRF shorter than 4.4 Kb and (%*Hpa*II-TRF - %*Msp*I-TRF)/%*Hpa*II-TRF for the TRF longer than 9.4 Kb (Table 2, Figure 5). The subtelomeres of short telomeres turned out to be proportionally hypomethylated in female PD patients. In summary, these data showed that long telomeres decreased and the subtelomeric regions of short telomeres were hypomethylated in PD in female PD patients but not in male patients.

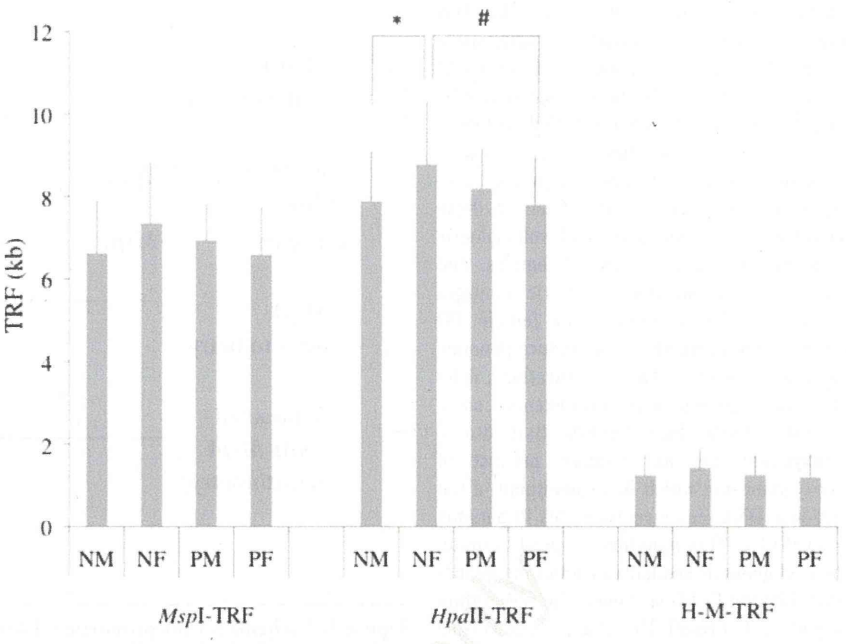

Figure 1. The mean *Msp*I-TRF (telomere length), *Hpa*II-TRF (methylated telomere length) and *Hpa*II-*Msp*I-subtracted length (H-M; subtelomeric methylated range) of the healthy control participants and the Parkinson's patients. Vertical bars depict the standard deviations. Abbreviations: NM, normal males; NF normal females; PM Parkinson's males; PF Parkinson's females. *# P<0.05; *Gender-related difference; #Parkinson's disease-related difference.

Discussion

Telomere length shortening with aging can be enhanced by various human pathophysiological conditions. The analysis of a telomerase-deficient mouse mutants have indicated that telomere shortening affects the neighboring subtelomeric hypomethylation and that shortened telomeres are associated with subtelomeric hypomethylation.[10] In addition, mutations in DNA methyltransferase (DNMT3B) in humans lead to autosomal recessive ICF (immunodeficiency, centromeric region instability, facial anomalies) syndrome.[19] The telomeres of the somatic cells in patients with the syndrome are abnormally short.[20] Therefore, the hypomethylated state of subtelomeric regions is thought to result in telomere shortening. The present study showed that the long telomeres decreased and the short telomeres with methylated subtelomeres decreased in PD patients, but these PD-associated telomeric

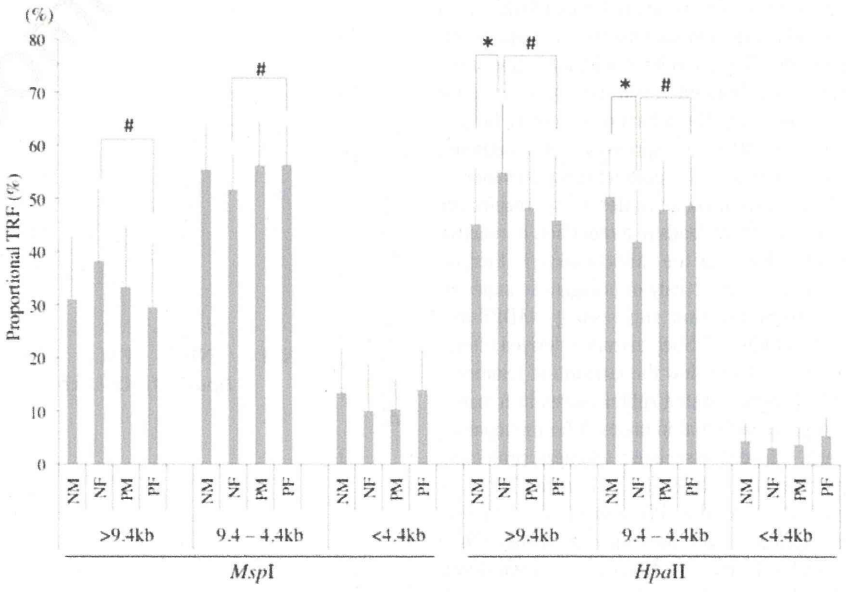

Figure 2. The distribution of methylation-insensitive (*Msp*I)- and -sensitive (*Hpa*II)-TRF lengths in the healthy controls and the Parkinson's patients. Telomere fragment length percentage profiles of long (>9.4 Kb), intermediate (9.4-4.4 Kb) and short (<4.4 Kb) length ranges are shown. The densitometry was examined for both cases of *Msp*I and *Hpa*II digestion. The abbreviations are similar to those in Figure 1. *#P<0.05; *Gender-related difference; #Parkinson's disease-related difference.

changes were observed only in females. Our previous studies demonstrated the aging-associated changes in the telomere of peripheral leukocytes of healthy Japanese subjects, that is, long telomeres with hypomethylated subtelomeres decrease and short telomeres with hypomethylated subtelomere increase with age.[21] In the present study, some of these aging-associated telomeric and subtelomeric changes were detected in PD females, and these aging-associated telomeric changes seemed to be accelerated in female PD patients. Oxidative stress can induce genomic mutations including base modifications, deletions and rearrangements.[22] For example, some recent reports have shown that 8-oxo-deoxyguanosine, an oxidized product of deoxyguanosine which is a constituent of the genomic DNA sequence, increases in patients with PD.[23-25] This mutation can lead to mutations of genomic sequences containing guanosine, like the CCGG sequence, the recognition site of *Msp*I or *Hpa*II. This change is detectable by the method introduced in the present study. Such a mutation inhibits genomic methylation, because the DNA methyltransferases cannot react with the mutated DNA, so the mutated region remains unmethylated.[26] Such interference with the methyltransferase activity may result in telomeric and subtelomeric hypomethylation. An enhancement of the oxidative stress may therefore yield not only an acceleration of telomeric erosion but also telomeric and subtelomeric hypomethylation. For this reason, the enhanced oxidative stress may be followed possibly by accelerated telomere attrition and genomic hypomethylation in the telomeric and subtelomeric regions in PD patients. The age-related telomere shortening can be ameliorated by estrogen, because estrogen augments the telomerase activity by promoting *TERT* gene expression.[27] Furthermore, estrogen has been reported to prevent superoxide production via activation of the respiratory function, which leads to a reduction of reactive oxygen leaks in the mitochondria,[28] thereby, increasing the activity of manganese superoxide dismutase and suppressing NADPH-oxidase activity.[29-31] Such estrogen-derived effects are expected to slow the attrition of telomeres with hypomethylated subtelomeres in females, compared with that in males. After menopause, such estrogen-associated telomere protecting mechanisms will decline with aging. This may explain why the PD-associated telomeric changes are more prominent in females than in males. In addition, Kikuchi *et al.* have shown that the level of an oxidized DNA product, 8-hydroxy-2'-deoxyguanosine, is higher in female PD patients, but not in male PD patients, in comparison to controls.[23] These results indicate that disease conditions can affect the telomere structure in a gender-associated manner. The correlation between the

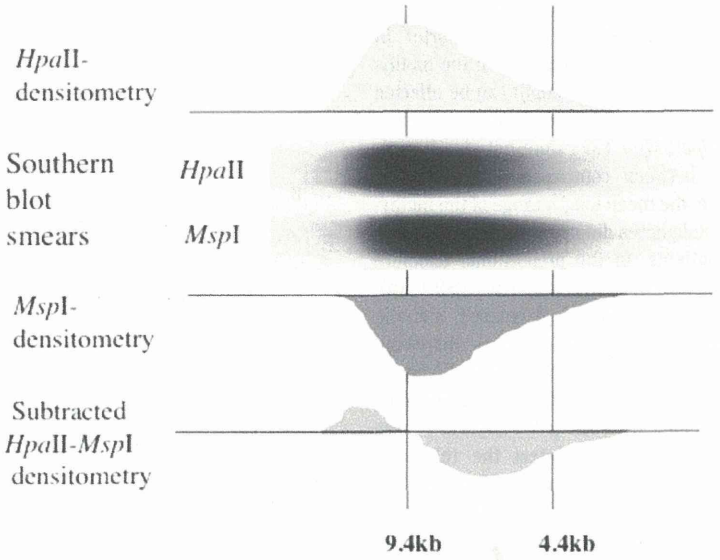

Figure 3. A schema for the proportional densitometric analysis of the isoschizomeric TRFs of *Msp*I- and *Hpa*II-digest. The densitometry data were divided into three parts, >9.4 Kb, 9.4-4.4 Kb, and <4.4 Kb. A representative genomic Southern blot of leukocyte DNA with telomere probe using *Msp*I and *Hpa*II and the analysis of the *Hpa*II-*Msp*I-subtracted TRF distribution. Densitometric curves are shown above or below the Southern blot smear results. A subtracted distribution pattern calculated from subtraction of the two densitometries is shown below.

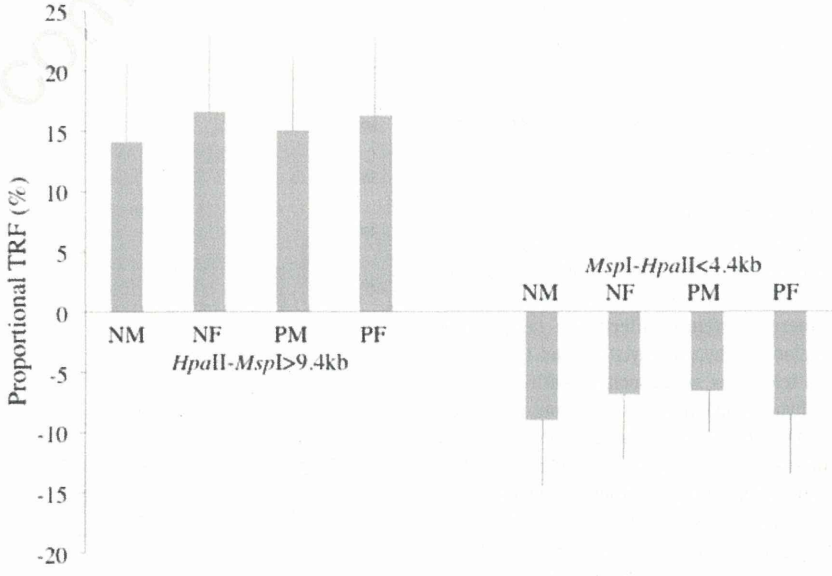

Figure 4. The subtracted distribution of methylation-insensitive (*Msp*I)- and methylation–sensitive (*Hpa*II)-TRF lengths in the healthy controls and in the Parkinson's patients. The subtracted value of the *Msp*I-TRF densitometry from the *Hpa*II-TRF densitometry in the subdivided parts (>9.4kb, <4.4kb) are shown as columns. The percentage of the respective area was presented as the fraction of the whole densitometric area (set as 100%). The abbreviations are similar to those in Figure 1.

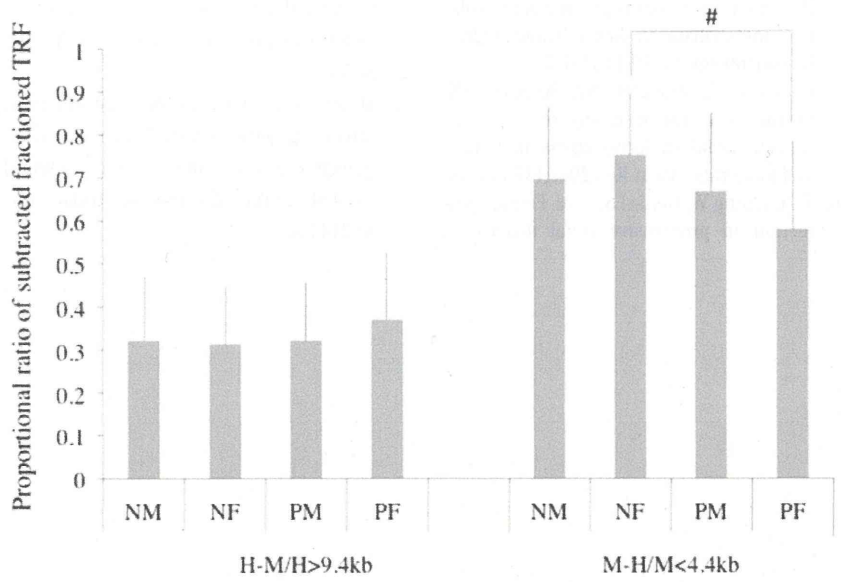

Figure. 5 The relative methylation status of subtelomeres of long (>9.4 Kb) and short (<4.4 Kb) telomere length ranges in controls and PD patients. Ratio of the subtracted percentage of *Hpa*II-*Msp*I *vs* percentage of *Hpa*II >9.4 Kb ((*Hpa*II-*Msp*I)/*Hpa*II (>9.4 Kb)) and that of *Msp*I-*Hpa*II *vs* *Msp*I <4.4 Kb ((*Msp*I-*Hpa*II)/*Msp*I (<4.4 Kb)) are used as indices indicating the subtelomeric methylation of longer (than 9.4 Kb) and shorter (than 4.4 Kb) telomeres, respectively. Vertical bars depict the standard deviations. #P<0.05.

attrition rate of a telomere and its subtelomeric hypomethylation range in individuals should be elucidated in a cohort study. The present study also showed that the analysis of the telomere length distribution and subtelomeric methylation status is more useful to detect disease-associated telomeric changes than an analysis of the mean TRF measurement. However, we could not clarify why the PD-associated telomeric changes could be observed only in the telomere length distribution and in the subtelomeric methylation status. The simple influence of oxidative stress on the telomere structure described above cannot explain this finding. Further investigation is necessary to determine the fate of cells bearing short, intermediate, and long telomeres. Further studies are also required to confirm the involvement of the disease-related subtelomeric methylation state in the telomeric shortening process in a cell.

Reference

1. Blackburn EH. Structure and function of telomeres. Nature (London) 1991;350:569-73.
2. Zakian VA. Telomeres: beginning to understand the end. Science 1995;270:1601-7.
3. Guan JZ, Maeda T, Sugano M, et al. Change in the telomere length distribution with age in the Japanese population. Mol Cell Biochem 2007;304:253-60.
4. Okuda K, Khan MY, Skurnick J, et al. Telomere attrition of the human abdominal aorta: relationships with age and atherosclerosis. Atherosclerosis 2000;152:391-8.
5. Uziel O, Singer JA, Danicek V, et al. Telomere dynamics in arteries and mononuclear cells of diabetic patients: effect of diabetes and of glycemic control. Exp Gerontol 2007;42:971-8.
6. Panossian LA, Porter VR, Valenzuela HF, et al. Telomere shortening in T cells correlates with Alzheimer's disease status. Neurobiol ageing 2003;24:77-84.
7. Valdes AM, Andrew T, Gardner JP, et al. Obesity, cigarette smoking, and telomere length in women. Lancet 2005;366:662-4.
8. Epel ES, Blackburn EH, Lin F, et al. Accelerated telomere shortening in response to life stress. Proc Natl Acad Sci USA 2004;101:17312-5.
9. Guan JZ, Maeda T, Sugano M, et al. An analysis of telomere length in sarcoidosis. J Gerontol A Biol Sci Med Sci 2007;62:1199-203.
10. Benetti R, García-Cao M, Blasco MA. Telomere length regulates the epigenetic status of mammalian telomeres and subtelomeres. Nat Genet 2007;39:243-50.
11. Petrozzi L, Lucetti C, Gambaccini G, et al. Cytogenetic analysis oxidative damage in lymphocytes of Parkinson's disease patients. Neurol Sci 2001;22:83-4.
12. Gao HM, Liu B, Zhang W, Hong JS. Novel anti-inflammatory therapy for Parkinson's disease. Trends Pharmacol Sci 2003;24:395-401.
13. Beal MF. Mitochondria, oxidative damage, and inflammation in Parkinson's disease. Ann NY Acad Sci 2003;991:120-31.
14. Hirsch EC, Breidert T, Rousselet E, et al. The role of glial reaction and inflammation in Parkinson's disease. Ann NY Acad Sci 2003;991:214-28.
15. McGeer PL, Yasojima K, McGeer EG. Inflammation in Parkinson's disease. Adv Neurol 2001;86:83-9.
16. Wang H, Chen H, Gao X, et al. Telomere length and risk of Parkinson's disease. Mov Disord 2008;23:302-5.
17. Eerola J, Kananen L, Manninen K, et al. No evidence for shorter leukocyte telomere length in Parkinson's disease patients. J Gerontol A Biol Sci Med Sci 2010;65:1181-4.
18. Watfa G, Dragonas C, Brosche T, et al. Study of telomere length and different markers of oxidative stress in patients with Parkinson's disease. J Nutr Health Aging 2011;15:277-81.
19. Hansen RS, Wijmenga C, Luo P, et al. The DNMT3B DNA methyltransferase gene is mutated in the ICF immunodeficiency syndrome. Proc Natl Acad Sci USA 1999;96:14412-7.
20. Yehezkel S, Segev Y, Viegas-Péquignot E, et al. Hypomethylation of subtelomeric regions in ICF syndrome is associated with abnormally short telomeres and enhanced transcription from telomeric regions. Hum Mol Genet 2008;17:2776-89.
21. Maeda T, Guan JZ, Oyama J, et al. Age-related changes in subtelomeric methylation in the normal Japanese population. J Gerontol A Biol Sci Med Sci 2009;64:426-34.
22. Franco R, Schoneveld O, Georgakilas AG, Panayiotidis MI. Oxidative stress, DNA methylation and carcinogenesis. Cancer Lett 2008;266:6-11.
23. Kikuchi A, Takeda A, Onodera H, et al. Systemic increase of oxidative nucleic acid damage in Parkinson's disease and multiple system atrophy. Neurobiol Dis 2002;9:244-8.
24. Chen CM, Liu JL, Wu YR, et al. Increased oxidative damage in peripheral blood correlates with severity of Parkinson's disease. Neurobiol Dis 2009;33:429-35.
25. Seet RC, Lee CY, Lim EC, et al. Oxidative damage in Parkinson disease: measurement using accurate biomarkers. Free

Radic Biol Med 2010;48:560-6.
26. Wachsman JT. DNA methylation and the association between genetic and epigenetic changes: relation to carcinogenesis. Mutat Res 1997;375:1-8.
27. Kyo S, Takakura M, Kanaya T, et al. Estrogen activates telomerase. Cancer Res 1999;59:5917-21.
28. Irwin RW, Yao J, Hamilton RT, et al. Progesterone and estrogen regulate oxidative metabolism in brain mitochondria. Endocrinology 2008;149:3167-75.
29. Razmara A, Duckles SP, Krause DN, Procaccio V. Estrogen suppresses brain mitochondrial oxidative stress in female and male rats. Brain Res 2007;1176:71-81.
30. Ji H, Zheng W, Menini S, et al. Female protection in progressive renal disease is associated with estradiol attenuation of superoxide production. Gend Med 2007;4: 56-71.
31. Miller AA, Drummond GR, Mast AE, et al. Effect of gender on NADPH-oxidase activity, expression, and function in the cerebral circulation: role of estrogen. Stroke 2007; 38:2142-9.

International Journal of Radiation Biology, 2012; Early Online: 1–4

ISSN 0955-3002 print / ISSN 1362-3095 online
DOI: 10.3109/09553002.2013.734945

informa
healthcare

Radiation-associated changes in the length of telomeres in peripheral leukocytes from inpatients with cancer

Toyoki Maeda[1], Katsumasa Nakamura[2], Kazushige Atsumi[3], Masakazu Hirakawa[3], Yasuko Ueda[1] & Naoki Makino[1]

[1]*Department of Cardiovascular, Respiratory and Geriatric Medicine, Kyushu University Beppu Hospital, Beppu, Oita,* [2]*Department of Clinical Radiology, Graduate School of Medical Sciences, Kyushu University, Fukuoka, and* [3]*Department of Radiology, Kyushu University Beppu Hospital, Beppu, Oita, Japan*

Abstract

Purpose: **The telomere length of somatic cells shortens with age and with other endogenous and exogenous pathogenic factors. However, the effects of radiation therapy on telomere DNA of non-cancer tissue have not been thoroughly investigated. This study analyzed the telomere length of inpatients with cancer treated with radiation therapy to see whether the telomere lengths change in response to therapeutic radiation.**

Materials and methods: **Twenty-five patients were enrolled in the study. The patients had lung cancer, prostate cancer, thyroid cancer, hepatoma, or rectal cancer. They received radiation therapy with a dose range of 15–74 Gy. The telomere lengths and telomere length distribution in peripheral leukocytes were analyzed by using a Southern blot-based method.**

Results: **The telomere length and the telomere length distribution of the peripheral leukocytes did not change after radiation therapy. However, there was a significant proportional decrease in the short telomere fraction (< 4.4 kb) per day and per Gy.**

Conclusions: **This observation suggested that the telomere length distribution of peripheral leukocytes could be affected by radiation therapy, and that the effect of radiation tends to appear in cells with short telomeres. Radiation therapy-associated somatic telomere length change within a short range of time, about three months or shorter, can be detected by analyzing the mean telomere length and telomere length distribution.**

Keywords: Radiotherapy, telomeres, clinical radiobiology

Introduction

The telomere is the terminal structure of a chromosome, containing a repetitive sequence. The length of telomeres in dividing somatic cells becomes gradually shorter because of the inability of DNA replication from the 3′-end (McEachern et al. 2000). This shortening is associated with various endogenous and exogenous pathogenic factors including aging, smoking, mental stress, and a clinical history of ischemic heart disease, diabetes mellitus, and Alzheimer's disease (Brouilette et al. 2003, Panossian et al. 2003, Epel et al. 2004, Ogami et al. 2004, Valdes et al. 2005, Uziel et al. 2007). Radiation can also affect the telomere attrition of somatic cells (Sgura et al. 2006, Belloni et al. 2011). Radiation therapy is a powerful therapeutic procedure for localized cancer lesions, but the normal tissue surrounding the cancer lesion can be still affected (Zelefsky et al. 2000). Radiation causes somatic mutations. Furthermore, there is increased chromosomal abnormality in circulating lymphocytes after radiation therapy for a localized cancer (Hartel et al. 2010). These reports lead to the hypothesis that some genomic regions, including telomeres, in circulating leukocytes can be affected by radiation therapy. This study investigated the genomic effects of radiation therapy (RadT) on telomere attrition in cancer treatment by analyzing the telomere length in patients' peripheral leukocytes.

Materials and methods

Patients

Twenty-five patients (19 males and six females) with cancer, that were admitted to Kyushu University Beppu Hospital for radiation therapy from 2010 April to 2011 September, were enrolled. The profile of all patients receiving radiation therapy is shown in Table I. There were 16 patients with lung cancer, five with thyroid cancer, two with prostate cancer, one with rectal cancer and one with hepatoma. The age range of the patients receiving radiation therapy was from 52–83 years old. The mean radiation dose was 52.0 Gy. The radiation dose ranged from 15–74 Gy. The radiation therapeutic period ranged from 4–97 days. Twenty-two inpatients (11 males and 11 females) with non-cancer disease were also enrolled as control subjects. The control subjects included patients with cerebrovascular disease, Parkinson's disease, spinocerebellar degeneration, lumbar spondylosis, and rheumatoid arthritis admitted for physical therapy for the subacute or

Correspondence: Dr Toyoki Maeda, Department of Cardiovascular, Respiratory and Geriatric Medicine, Kyushu University Beppu Hospital, 4546 Tsurumihara, Beppu, Oita, 874-0838, Japan. Tel: +81 977 27 1676. Fax: +81 977 27 1682. E-mail: maedat@beppu.kyushu-u.ac.jp

(Received 4 April 2012; revised 27 July 2012; accepted 2 September 2012)

Table I. The profile of patients with cancer and the radiation therapy.

Patient number	The site of cancer	Gender	Age (y.o)	Period (days)	Dose (Gy)
1	Thyroid	F	73	33	60
2	Prostate	M	77	51	70
3	Thyroid	M	52	45	60
4	Lung	M	76	47	60
5	Lung	F	81	45	60
6	Lung	M	75	14	30
7	Rectum	F	80	4	15
8	Lung	M	75	10	48
9	Prostate	M	67	45	74
10	Thyroid	M	68	97	30
11	Liver	M	60	14	48
12	Lung	M	68	45	60
13	Lung	F	76	28	50
14	Lung	M	66	4	48
15	Lung	M	70	4	48
16	Lung	F	74	4	48
17	Lung	M	80	9	48
18	Lung	M	65	42	60
19	Lung	M	66	54	64
20	Thyroid	M	60	49	54
21	Lung	M	83	45	60
22	Thyroid	F	80	43	60
23	Lung	M	83	4	48
24	Lung	M	79	10	48
25	Lung	M	78	7	48

y.o., years old; Period, Total radiation therapy period; Dose, Total radiation dose; M, male; F, female.

the chronic stage of their diseases. The present research was approved by the Conjoint Health Research Ethics Board of Kyushu University, and written consent was obtained from all the participants.

Telomere length (TL) analysis

DNA samples were obtained from peripheral leukocytes of the patients. Blood samples were collected from the patients at admission and at discharge. Blood samples were drawn, using heparinized syringes and 10 ml Vacutainer tubes (BD Diagnostics, Franklin Lakes, NJ, USA). The blood sample was diluted with 10 times the volume of 10 mM Tris-HCl, 1 mM sodium ethylenediaminetetraacetate (pH 8.0; Wako, Osaka, Japan) to remove erythrocytes by lowering the osmotic pressure. The peripheral leukocytes were collected by centrifugation.

Telomere detection was performed as previously described (Guan et al. 2007a, 2007b, Maeda et al. 2009). Blood cell DNA was extracted from samples and the DNA (0.1 μg) was digested with 1 U of *Msp*I restriction enzyme at 37°C (Promega KK, Tokyo, Japan) for 2 h. The digests (10 μl) were resolved by agarose gel-electrophoresis, and transferred by Southern blotting to a positively charged nylon membrane (Roche Diagnostics, Mannheim, Germany). The blotted DNA fragments were hybridized with a probe of 500 bp long (TTAGGG)n labeled with digoxigenin (Roche Japan, Tokyo, Japan). The membrane was then incubated with anti-digoxigenin-alkaline phosphatase-specific antibody (Roche Japan, Tokyo, Japan). The telomere probe was visualized by CSPD (disodium 3-(4-methoxy-spiro{1,2-dioxetane-3,2′-(5′-chloro) tri-cyclo[3.3.1.1]decan}-4-yl) phenyl phosphate; Boehringer Mannheim GmbH, Mannheim, Germany). The membrane was then exposed to Fuji XR film with an intensifying screen (Fujifilm Corporation, Tokyo, Japan). The smears of the autoradiogram were captured on an Image Master (Trioptics Japan, Shizuoka, Japan), and the telomere length was then assessed quantitatively. Every sample was measured in triplicate.

Telomere length (TL) distribution was analyzed by comparing the telomere length using a telomere percentage analysis with three intervals of length as defined by a molecular weight standard, as previously described (Guan et al. 2007b). The intensity (photo-stimulated luminescence [PSL]) of each telomeric sample was divided into grid squares according to the molecular size ranges of HindIII-digested lambda phage genomic DNA used as a molecular weight standard: >9.4 kb, 9.4–4.4 kb, and <4.4 kb. The percentage of PSL in each molecular weight range was measured (% PSL = intensity of a defined region-background $\times 100$/total lane intensity-background). Peak TL were used as representatives of TRF (Terminal Restriction Fragment Length) in this study.

Statistical analysis

The normality of the data was examined using the Kolmogorov-Smirnov test and the homogeneity of variance by using the Levene Median test. The difference in the mean TL and a telomere percentage analysis with age, gender and other factors were analyzed using a two-way analysis of variance (ANOVA) test followed by all pairwise multiple comparison procedures using Tukey's post-hoc test. Logarithmic or square-root transformations were used to normalize the data for fitting into the two-way ANOVA, if the normality and variance of the data were not acceptable in the first test. The data are presented as the mean ± standard deviation bars. The criterion for significance is $p<0.05$. All analyses were carried out using the Sigma Statistical Analysis software package (Sigma 2.03, 2001; Sigma, St Louis, MO, USA).

Results

The telomeric parameters of patients at the time of admission are shown in Table II. There was no difference in the gender distribution between RadT patients (cancer patients) and non-RadT patients (control). There was no significant difference of the mean TL and the TL distribution at admission between cancer patients and age-matched controls. The change in telomeric length parameters during the hospitalized period was compared. The proportion of TL fractions at admission and at discharge was compared between RadT

Table II. The telomere length (TL) parameters of patients at admission.

	Patients with cancer for RadT	Patients with no cancer	*p*-value/ RadT vs. NRadT
Radiation (Gy)	52.0 ± 12.8	-	-
Number of M and F	19 (M) and 6 (F)	11 (M) and 11 (F)	0.070
Age (years old)	72.5 ± 8.0	70.5 ± 19.8	0.668
TL (kb)	5.9 ± 0.5	6.0 ± 0.8	0.894
>9.4 kb (%)	22.4 ± 6.1	23.7 ± 9.2	0.578
4.4–9.4 kb (%)	59.5 ± 4.9	57.6 ± 5.4	0.225
4.4 kb> (%)	18.1 ± 6.4	18.7 ± 7.1	0.780

M, male; F, female; RadT, radiation therapy; NRadT, non-radiation therapy. The values are presented as the mean value ± standard deviation. $N=25$ for patients for RadT. $N=22$ for patients for patients with no cancer.

Table III. The ratio of the patients' telomere lengths (TL) between admission and at discharge.

	Discharge/Admission				
	RadT	*p*-value/ RadT vs. 1	NRadT	*p*-value/ NRadT vs. 1	*p*-value/ RadT vs. NRadT
TL	1.03 ± 0.08	0.219	1.00 ± 0.09	0.880	0.597
>9.4 kb	1.07 ± 0.18	0.961	1.03 ± 0.22	0.581	0.692
4.4–9.4 kb	1.00 ± 0.06	0.284	0.98 ± 0.09	0.239	0.110
<4.4 kb	0.92 ± 0.18	0.227	1.09 ± 0.51	0.439	0.248

RadT, radiation therapy; NRadT, non-radiation therapy. The values are presented as the mean value ± standard deviation. $N = 25$ for patients for RadT. $N = 22$ for patients for NRadT. '1' of 'RadT vs. 1' refers to no change of the corresponding value between at admission and at discharge, in which the value at admission and that at discharge are the same, and the proportion between them is 1.

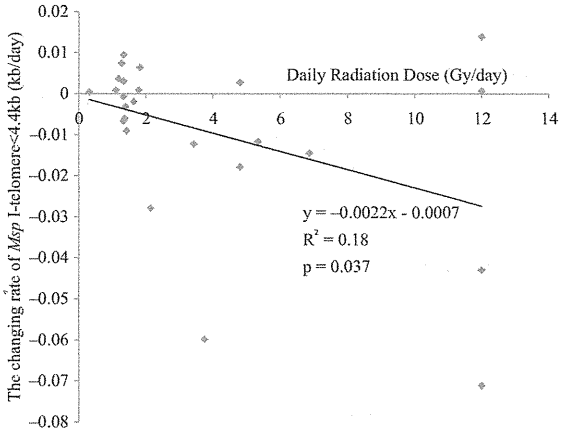

Figure 1. The change in the proportion of the short telomere length fraction with daily radiation dose. Each point represents a single patient. There were 25 irradiated patients and their profiles are summarized in Table I.

patients and controls. There was no radiation-associated difference in the TL distribution (Table III). The radiation period varied among RadT patients, and this variation might be one of factors diversifying radiation-associated changes in the telomeric parameters. Therefore, the daily change rate of telomeric parameters was compared. The mean TRF of RadT patients increased significantly ($p = 0.0241$), and the short telomeres <4.4 kb decreased significantly in RadT patients ($p = 0.0337$; Table IV). Moreover, the daily radiation dose correlated to the decreasing rate of short (<4.4 kb) telomeres of RadT patients (Figure 1).

Discussion

Radiation therapy apparently had no effect on the TL and the TL distribution in circulating leukocytes during the radiation period. However, the TL-change rate per day was reflected in a decreasing proportion of short-ranged telomeres in association with radiation therapy. Individual somatic TL changes were detectable even within a short period of a few weeks or a few months in clinical cases. The radiation-associated effect on TL distribution was observed only in the short telomeres (<4.4 kb) but not in long (>9.4 kb) and intermediate-sized (4.4–9.4 kb) telomeres. Radiation therapy seemed to exclusively affect short telomeres. There are two possible explanations for these changes in TL. One is that only short telomeres were subjected to a telomere-elongating mechanism. The other was that short telomeres tended to disappear from the TL distribution. Both possibilities could contribute to the increase of the mean TL observed in Table IV. Radiation has been reported to activate telomerase in cultured cells, and this results in telomere elongation and a cellular hormesis effect (Richardson 2009). This seems to be applicable to the former case. However, the endogenous telomerase expression in normal cells is detectable in limited types of cells, such as stem cells and germ-line cells, and the other intact somatic cells express telomerase at an undetectable level (Blasco 2005). It would also be impossible to distinguish whether cells with long telomeres or those with short telomeres, expresses telomerase, even if the telomerase activity in circulating leukocytes could be detected. However, the mechanism can be determined by analyzing the changes in TL distribution. Elongated telomeres originally derived from short telomeres would shift to the longer fraction if there was a telomere elongating mechanism; therefore, the loss of short telomeres would to an increase of long telomeres, resulting in a reciprocal increasing tendency of 4.4–9.4 kb in contrast to the decrease of short telomeres (<4.4 kb). The disappearance of short telomeres would contribute to a relatively homogeneous increase of long and intermediate-sized telomeres. The current result was more consistent to the latter case than to the former case, based on the results shown in Table IV. Increased radiation sensitivity is seen with telomere shortening (Ayouaz et al. 2008, Drissi et al. 2011); therefore, aged cells bearing accumulate genomic mutations and short telomeres in a radiosensitive cell subpopulation enter a senescent state and tend to decrease during radiation therapy. Radiotherapy is an effective anti-cancer therapeutic procedure. However, radiotherapy can affect the surrounding normal tissue, though the effects may be minimal. The current study found no gross RadT-effect on TL, but there was a decrease in the fraction of short telomeres, probably representing the loss of cells bearing short telomeres. Moreover, the extent of the decrease of the short telomere fraction was

Table IV. The changing ratios per day of the patients' telomere lengths (TL).

	RadT ($N = 25$)		NRadT ($N = 22$)		RadT vs. NRadT
	Av ± SD	*p*-value/vs. 0	Av ± SD	*p*-value/ vs. 0	*p*-value
TL	0.0023 ± 0.0048	0.024	3.0×10^{-6} ± 0.0030	0.996	0.053
>9.4 kb	0.0016 ± 0.016	0.602	0.00053 ± 0.0055	0.661	0.741
4.4–9.4 kb	0.0018 ± 0.0064	0.171	−0.00049 ± 0.0023	0.335	0.105
<4.4 kb	−0.0094 ± 0.021	0.034	0.0040 ± 0.023	0.429	0.045

RadT, radiation therapy; NRadT, non-radiation therapy. The values are presented as the mean value ± standard deviation.

correlated with the daily radiation dose. Therefore, RadT has effects on the nuclear DNA of circulating leukocyte evidenced by a decreasing proportion of cells with short telomeres. The change of the TL distribution turned out to be a parameter that was sufficiently sensitive to detect radiation-associated genotoxic effects. The current results should be reconfirmed by further study of a larger number of subjects.

Acknowledgements

We are grateful to Brian Quinn for his linguistic advice on the manuscript.

Declaration of interest

The authors report no conflicts of interest. The authors alone are responsible for the content and writing of the paper.

This work was supported by a grant from the Ministry of Education, Science, and Culture of Japan (#23590885)

References

Ayouaz A, Raynaud C, Heride C, Revaud D, Sabatier L. 2008. Telomeres: Hallmarks of radiosensitivity. Biochimie 90:60–72.

Belloni P, Latini P, Palitti F. 2011. Radiation-induced bystander effect in healthy G0 human lymphocytes: Biological and clinical significance Mutation Research 713:32–38.

Blasco MA. Telomeres and human disease: Ageing, cancer. and beyond. 2005. Nature Reviews Genetics 6:611–622.

Brouilette S, Singh RK, Thompson JR, Goodall AH, Samani NJ. 2003. White cell telomere length and risk of premature myocardial infarction. Arteriosclerosis, Thrombosis, and Vascular Biology 23: 842–846.

Drissi R, Wu J, Hu Y, Bockhold C, Dome JS. 2011. Telomere shortening alters the kinetics of the DNA damage response after ionizing radiation in human cells. Cancer Prevention Research (Philadelphia, PA) 4:1973–1981.

Epel ES, Blackburn EH, Lin J, Dhabhar FS, Adler NE, Morrow JD, Cawthon RM. 2004. Accelerated telomere shortening in response to life stress. Proceedings of the National Academy of Sciences of the USA 101:17312–17315.

Guan JZ, Maeda T, Sugano M, Oyama J, Higuchi Y, Suzuki T, Makino N. 2007a. An analysis of telomere length in sarcoidosis. The Journals of Gerontology Series A Biological Sciences and Medical Sciences 62:1199–1203.

Guan JZ, Maeda T, Sugano M, Oyama J, Higuchi Y, Makino N. 2007b. Change in the telomere length distribution with age in the Japanese population. Molecular Cellular Biochemistry 304:253–260.

Hartel C, Nikoghosyan A, Durante M, Sommer S, Nasonova E, Fournier C, Lee R, Debus J, Schulz-Ertner D, Ritter S. Chromosomal aberrations in peripheral blood lymphocytes of prostate cancer patients treated with IMRT and carbon ions. Radiotherapy. and Oncology 2010;95:73–78.

Maeda T, Guan JZ, Oyama J, Higuchi Y, Makino N. 2009. Age-related changes in subtelomeric methylation in the normal Japanese population. The Journals of Gerontology Series A Biological Sciences and Medical Sciences 64:426–434.

McEachern MJ, Krauskopf A, Blackburn EH. 2000. Telomeres and their control. Annual Review of Genetics 34:331–358.

Ogami M, Ikura Y, Ohsawa M, Matsuo T, Kayo S, Yoshimi N, Hai E, Shirai N, Ehara S, Komatsu R, Naruko T, Ueda M. 2004. Telomere shortening in human coronary artery diseases. Arteriosclerosis, Thrombosis, and Vascular Biology 24:546–550.

Panossian LA, Porter VR, Valenzuela HF, Zhu X, Reback E, Masterman D, Cummings JL, Effros RB. 2003. Telomere shortening in T cells correlates with Alzheimer's disease status. Neurobiology of Ageing 24:77–84.

Richardson RB. 2009. Ionizing radiation and aging: Rejuvenating an old idea. Aging (Albany NY) 1:887–902.

Sgura A, Antoccia A, Berardinelli F, Cherubini R, Gerardi S, Zilio C, Tanzarella C. 2006. Telomere length in mammalian cells exposed to low- and high-LET radiations. Radiation Protection Dosimetry 122:176–179.

Uziel O, Singer JA, Danicek V, Sahar G, Berkov E, Luchansky M, Fraser A, Ram R, Lahav M. 2007. Telomere dynamics in arteries and mononuclear cells of diabetic patients: Effect of diabetes and of glycemic control. Experimental Gerontology 42:971–978.

Valdes AM, Andrew T, Gardner JP, Kimura M, Oelsner E, Cherkas LF, Aviv A, Spector TD. 2005. Obesity, cigarette smoking, and telomere length in women. The Lancet 366:662–664.

Zelefsky MJ, Fuks Z, Happersett L, Lee HJ, Ling CC, Burman CM, Hunt M, Wolfe T, Venkatraman ES, Jackson A, Skwarchuk M, Leibel SA. 2000. Clinical experience with intensity modulated radiation therapy (IMRT) in prostate cancer. Radiotherapy and Oncology 55:241–249.

Aging Clin Exp Res (2013) 25:17–23
DOI 10.1007/s40520-013-0006-0

ORIGINAL ARTICLE

Analysis of telomere length and subtelomeric methylation of circulating leukocytes in women with Alzheimer's disease

Jing-Zhi Guan · Wei Ping Guan · Toyoki Maeda · Naoki Makino

Received: 6 October 2011 / Accepted: 22 November 2011 / Published online: 3 April 2013

Abstract
Backgrounds and aims Telomere attrition proceeds with the aging process, and is also associated with aging disease conditions, such as Alzheimer's disease (AD). The aging process also affects subtelomeric methylation status. In the present study, the telomere length and the subtelomeric methylation status in female AD patients were analyzed to see how AD affects telomere structure.
Methods Terminal restriction fragment length of 23 AD patients' peripheral leukocytes was analyzed with methylation sensitive- and insensitive-isoschizomer by Southern blot.
Results AD patients were found to have normal mean telomere lengths (controls; 6.4 ± 0.9 kb, AD; 6.1 ± 0.8 kb, $p = 0.131$), a proportionally decreased number of the longest telomeres (>9.4 kb) (controls; 30.3 ± 7.9 %, AD; 24.4 ± 8.3 %, $p = 0.013$), increased medium-sized telomeres (controls; 51.7 ± 3.3 %, AD 55.5 ± 6.4 %, $p = 0.015$) and unchanged numbers of the shortest telomeres (<4.4 kb) (controls; 18.0 ± 7.8, AD; 20.2 ± 8.9 %, $p = 0.371$) in their peripheral leukocytes. The subtelomeres of telomeres in the shortest range (<4.4 kb) were more methylated in AD subjects than in controls (controls; 0.21 ± 0.23, AD; 0.41 ± 0.26, $p = 0.016$).
Conclusions These results may indicate that AD contributes to the loss of cells bearing the shortest telomeres, with hypomethylation of subtelomeres occurring in addition to telomere attrition, resulting in an apparent normal mean telomere length in AD patients. The relatively high subtelomeric methylation status of the shortest telomeres in peripheral blood leukocytes may be a characteristic of AD. This report demonstrates that the epigenetic status of the telomeric region is affected by disease conditions.

Keywords Alzheimer's disease · DNA methylation · Female gender · Subtelomere · Telomere

Introduction

A telomere is a structure consisting of repetitive DNA sequences and accessory peptide factors located at the termini of human chromosomes [1, 2]. Telomeres protect genomic DNA from exonuclease attacks or end-to-end DNA recombination between different chromosomes. Telomeres shorten gradually because of incomplete DNA duplication at the chromosome ends. This process is known as the 'end-replication problem'. An extremely shortened telomere stops mitosis and induces 'cell senescence'. Telomere attrition has been observed in peripheral blood nuclear cells with aging [3, 4]. Telomere length may be regarded as a biological clock of individuals. Older people have shorter telomeres in their somatic cells than young people do. In addition, telomere shortening is accelerated by various pathophysiological conditions, including physical stress, and disease conditions

J.-Z. Guan, W. P. Guan and T. Maeda contributed equally to this article.

J.-Z. Guan
309th Hospital of Chinese People's Liberation Army, Beijing 100091, China

W. P. Guan
Nanlou Neurology Department, Chinese PLA General Hospital, Beijing, China

T. Maeda (✉) · N. Makino
Division of Cardiovascular, Respiratory and Geriatric Medicine, Kyushu University Beppu Hospital, Beppu, Oita 874-0838, Japan
e-mail: maedat@beppu.kyushu-u.ac.jp